



TECHNICAL REPORT AMR-AE-04-01

VERIFICATION OF SIMULATION RESULTS USING SCALE MODEL FLIGHT TEST TRAJECTORIES

Jeff Obermark

Karla Key

**Aviation Engineering Directorate
Aviation and Missile Research, Development, and Engineering Center**

May 2004

Approved for public release; distribution is unlimited.

DESTRUCTION NOTICE

FOR CLASSIFIED DOCUMENTS, FOLLOW THE PROCEDURES IN DoD 5200.22-M, INDUSTRIAL SECURITY MANUAL, SECTION II-19 OR DoD 5200.1-R, INFORMATION SECURITY PROGRAM REGULATION, CHAPTER IX. FOR UNCLASSIFIED, LIMITED DOCUMENTS, DESTROY BY ANY METHOD THAT WILL PREVENT DISCLOSURE OF CONTENTS OR RECONSTRUCTION OF THE DOCUMENT.

DISCLAIMER

THE FINDINGS IN THIS REPORT ARE NOT TO BE CONSTRUED AS AN OFFICIAL DEPARTMENT OF THE ARMY POSITION UNLESS SO DESIGNATED BY OTHER AUTHORIZED DOCUMENTS.

TRADE NAMES

USE OF TRADE NAMES OR MANUFACTURERS IN THIS REPORT DOES NOT CONSTITUTE AN OFFICIAL ENDORSEMENT OR APPROVAL OF THE USE OF SUCH COMMERCIAL HARDWARE OR SOFTWARE.

REPORT DOCUMENTATION PAGE**Form Approved
OMB No. 074-0188**

Public reporting burden for this collection of information is estimated to average 1 hour per response, including the time for reviewing instructions, searching existing data sources, gathering and maintaining the data needed, and completing and reviewing this collection of information. Send comments regarding this burden estimate or any other aspect of this collection of information, including suggestions for reducing this burden to Washington Headquarters Services, Directorate for Information Operations and Reports, 1215 Jefferson Davis Highway, Suite 1204, Arlington, VA 22202-4302, and to the Office of Management and Budget, Paperwork Reduction Project (0704-0188), Washington, DC 20503

1. AGENCY USE ONLY**2. REPORT DATE**
May 2004**3. REPORT TYPE AND DATES COVERED**
Final; June 2001 to December 2004**4. TITLE AND SUBTITLE**Verification of Simulation Results Using
Scale Model Flight Test Trajectories**5. FUNDING NUMBERS****6. AUTHOR(S)**

Jeff Obermark

7. PERFORMING ORGANIZATION NAME(S) AND ADDRESS(ES)Commander
U. S. Army Research, Development, and Engineering Command
ATTN: AMSRD-AMR-AE-S-W
Redstone Arsenal, AL 35898**8. PERFORMING ORGANIZATION
REPORT NUMBER**

TR-AMR-AE-04-01

9. SPONSORING / MONITORING AGENCY NAME(S) AND ADDRESS(ES)**10. SPONSORING / MONITORING
AGENCY REPORT NUMBER****11. SUPPLEMENTARY NOTES****12a. DISTRIBUTION / AVAILABILITY STATEMENT**

Approved for public release; distribution is unlimited.

12b. DISTRIBUTION CODE

A

13. ABSTRACT (Maximum 200 Words)

The objective of this effort was to compare limited amounts of scale model trajectory data with appropriate full-scale data. The scale model data was scaled up to equivalent full-scale conditions. Two Degree-of-Freedom (2-DOF) trajectories and calculated miss-distances were compared to full-scale data. Likely error sources in the scale test process were identified. Simulation was used to estimate the effects of these errors on the trajectory. Simulation trends were used to estimate the scale trajectory without these errors. A second compromise scaling law was investigated as a possible improvement. For ejector-driven events at minimum sideslip, the most important variables for scale model construction are the mass moment of inertia and ejector forces. For these events, the pitch motion and resulting miss-distance calculations correspond well with the full-scale events. Additional testing is required to enable a thorough uncertainty analysis of the scale model test data, especially for sideslip conditions.

14. SUBJECT TERMS

Jettison, Froude Scaling, Scale Models, Store Separation, Helicopter

15. NUMBER OF PAGES

77

16. PRICE CODE**17. SECURITY CLASSIFICATION
OF REPORT**

UNCLASSIFIED

**18. SECURITY CLASSIFICATION
OF THIS PAGE**

UNCLASSIFIED

**19. SECURITY CLASSIFICATION
OF ABSTRACT**

UNCLASSIFIED

20. LIMITATION OF ABSTRACT

Unlimited

NSN 7540-01-280-5500

Standard Form 298 (Rev. 2-89)
Prescribed by ANSI Std. Z39-18
298-102

i/(ii Blank)

TABLE OF CONTENTS

	<u>Page</u>
I. INTRODUCTION	1
A. Background	1
B. Objective	1
C. Approach	1
II. DATA COLLECTION.....	2
A. Full-Scale Test.....	2
B. Half-Scale Test	2
C. Test Conditions	3
D. Test Equipment.....	3
III. ANALYSIS.....	7
A. Froude Scaling	7
B. Comparison	8
C. Discussion	11
D. Error Sources.....	12
E. Error Analysis.....	12
F. Error Correction	20
IV. CONCLUSIONS AND RECOMMENDATIONS	25
A. Conclusions.....	25
B. Recommendations.....	26
REFERENCES.....	27
ABBREVIATIONS.....	29
LIST OF SYMBOLS	31
APPENDIX A: TRAJECTORY DATA TABLES.....	A-1
APPENDIX B: TRAJECTORIES FROM OH-13 SCALE MODEL JETTISON TEST.....	B-1
APPENDIX C: VERTICAL MOTION AND PITCH MOTION COMPARISON FIGURES.....	C-1
APPENDIX D: COMPARISON OF PITCH MOTION CONDITIONS.....	D-1

TABLE OF CONTENTS (Cont.)

	<u>Page</u>
APPENDIX E: COMPARISON OF MISS-DISTANCE.....	E-1
APPENDIX F: DOWNWASH ON VERTICAL MOTION AND PITCH MOTION FIGURES	F-1
APPENDIX G: BASELINE SIMULATION RESULTS.....	G-1
APPENDIX H: EFFECT OF MOMENT OF INERTIA PLUS EJECTOR FORCE CORRECTION ON PITCH MOTION AND VERTICAL MOTION.....	H-1
APPENDIX I: EFFECT OF CORRECT MASS MOMENT OF INERTIA AND EJECTOR FORCES ON HALF-SCALE TEST DATA	I-1

LIST OF ILLUSTRATIONS

<u>Figure</u>	<u>Title</u>	<u>Page</u>
1.	Comparison of Scale Ejector Force Versus Froude Nominal Values	4
2.	Scale Model and Ejector Rack Installation	4
3.	ASVS Control Installation	5
4.	IRIG Installation	6
5.	Comparison of Vertical Motion at 40 Knots Full-Scale Conditions	9
6.	Comparison of Pitch Axis Motion at 40 Knots Full-Scale Conditions	10
7.	Calculated Miss-Distance Versus Time Curves at 40 Knots Full-Scale Conditions	11
8.	Simulation of Half-Scale Test, Vertical Motion, 40 Knots Full-Scale	13
9.	Simulation of Half-Scale Test, Pitch Motion, 40 Knots Full-Scale	14
10.	Effect of Mass Moment of Inertia on Vertical Motion, 40 Knots Full-Scale Conditions	15
11.	Effect of Mass Moment of Inertia on Pitch Motion, 40 Knots Full-Scale Conditions	15
12.	Effect of Ejector Force on Vertical Motion, 40 Knots Full-Scale Conditions	16
13.	Effect of Ejector Force on Pitch Motion, 40 Knots Full-Scale Conditions.....	17
14.	Effect of Lug Size on Vertical Motion, 40 Knots Full-Scale Conditions	17
15.	Effect of Lug Size on Pitch Motion, 40 Knots Full-Scale Conditions	18
16.	Effect of Mass Moment of Inertia and Ejector Forces on Vertical Motion, 40 Knots Full-Scale Conditions	19
17.	Effect of Mass Moment of Inertia and Ejector Forces on Pitch Motion, 40 Knots Full-Scale Conditions	19
18.	Effect of Ejector Forces and Mass Moment of Inertia on Half-Scale Vertical Motion Data, 40 Knots Full-Scale Conditions.....	20

LIST OF ILLUSTRATIONS (Cont.)

<u>Figure</u>	<u>Title</u>	<u>Page</u>
19.	Effect of Ejector Forces and Mass Moment of Inertia on Half-Scale Pitch Motion Data, 40 Knots Full-Scale Conditions.....	21
20.	Effect of Ejector Forces and Mass Moment of Inertia on Half-Scale Pitch Motion Data, 70 Knots Full-Scale Conditions.....	22
21.	Effect of Ejector Forces and Mass Moment of Inertia on Half-Scale Pitch Motion Data, 100 Knots Full-Scale Conditions.....	23
22.	Effect of Mass Moment of Inertia and Ejector Forces on Miss-Distance at 40 Knots Full-Scale Conditions.....	24

LIST OF TABLES

<u>Figure</u>	<u>Title</u>	<u>Page</u>
1.	Scale Model Test Conditions	3
2.	Scale Model Physical Properties	3
3.	Comparison Flight Conditions	8

I. INTRODUCTION

A. Background

The United States (U. S.) Army Aviation Engineering Directorate (AED) has the responsibility to determine airworthiness of externally mounted stores on Army helicopters. One portion of this airworthiness effort is the determination of safe clearance of separating stores. This determination can be made by direct test or through calculations, modeling, or simulation.

In order to enhance this process, the AED developed the Rotary Wing Stores Integration (RWSI) software as a part of the U.S. Air Force (AF) Seek Eagle Office (SEO) Weapons Modification and Simulation Capability (WMASC) project. The RWSI software simulates helicopter flight maneuvers and calculates the Six Degree-of-Freedom (6-DOF) trajectory and miss-distance of separating stores. The RWSI software was partially validated during development by comparing calculated results with test data for combinations of three aircraft and three stores.

B. Objective

In the case of store separation from helicopters, obtaining test data for clearance determination or for comparison to simulation data is expensive and time-consuming. As a result, weapon firing or jettison envelopes can be restricted due to lack of data. Also, a thorough validation of simulations and models of store separations is difficult due to lack of data.

The objective of this comparison is to determine if jettison of scale model stores from surrogate aircraft can represent the jettison of the real stores from Army helicopters. If this can be shown with a sufficient level of confidence, then testing methods for store separation can be changed. Jettison of scale model stores from surrogate aircraft can be accomplished faster and cheaper than the current test methodology using fleet-representative helicopters and real stores. This would increase the speed and decrease the cost of the airworthiness process. Additionally, large amounts of data can be obtained to validate simulations and models.

C. Approach

The approach for this comparison is to compare 6-DOF jettison trajectory data from a full-scale test with 6-DOF trajectory data from a test in which a scale model store was jettisoned from a surrogate helicopter. Because the jettison events are dominated by the force of the ejector racks, the Two Degree-of-Freedom (2-DOF) with the most movement are the 'Z' position (down) and the pitch angle. Although the test data includes all 6-DOF, these are the only two variables used in this comparison.

First, the half-scale results are scaled up to a corresponding full-scale trajectory using wind tunnel scaling laws. Then, the 2-DOF variables are compared directly. A second comparison is made by calculating the helicopter/store miss-distance using both the full-scale trajectory and the half-scale trajectory. This is a more realistic measure of the usefulness of the half-scale data since the goal of the analysis is to determine a safe clearance envelope for separation events.

II. DATA COLLECTION

A. Full-Scale Test

In order to validate the RWSI software, a test was conducted to collect trajectory data from firing and jettison events. Three different helicopter types and three types of stores were tested in various combinations [1]. The test conditions for the OH-58D helicopter, used in this analysis, are listed in Appendix A.

For this comparison, the trajectories obtained from an OH-58D helicopter jettisoning a M260 (7 tube) rocket launcher are used. The jettison events were filmed using high-speed (400 frames per second), film. The digitized film images were used in the Computer-Aided Store Separation Analysis System (CASSAS) software to extract the 6-DOF trajectories of each event. The trajectories from the full-scale test used in this comparison are tabulated in Appendix A. The trajectories were used as input to the Clearance and Collision Detection (CLRANC) software, which calculated a miss-distance versus time curve for each event.

B. Half-Scale Test

A flight test was conducted during June 1999, in which several half-scale model stores were jettisoned from an OH-13 helicopter. The purpose of the test was to determine the use-ability of the Airborne Separation Video System (ASVS). The ASVS is a ruggedized onboard digital camera and storage system that has been designed for use on Department of Defense (DOD) aircraft to record store separation events.

The half-scale model stores were designed to be scale models of the M260 rocket launcher. The weight, center of gravity, and moments of inertia of the scale launchers were chosen to comply with Froude scaling for half-scale models. The ejector used in this test was specially designed to deliver a force scaled in accordance with Froude scaling. The helicopter velocities were chosen to correspond with the Froude scaled velocities of the full-scale test.

These test events were filmed with high-speed, film and with the ASVS. The ASVS images were translated to an appropriate image format. These two types of images were used in the CASSAS software to extract the 6-DOF trajectories of each event. These trajectories were used as input to the CLRANC software, which calculated a miss-distance versus time curve for each event.

C. Test Conditions

The conditions for which data was collected in the scale model test are listed in the Table 1.

Table 1. Scale Model Test Conditions

<u>Drop No.</u>	<u>Date</u>	<u>Conditions</u>	<u>ASVS</u>	<u>Film</u>
1	15 Jun 00	15 Kts		X
2	15 Jun 00	15 Kts		X
3	15 Jun 00	20 Kts		X
4	16 Jun 00	30 kts	X	X
5	16 Jun 00	40 kts	X	X
6	16 Jun 00	50 kts	X	X
7	16 Jun 00	70 kts	X	X
8	16 Jun 00	Hover		X
9	16 Jun 00	Hover		X

The reduced 6-DOF trajectories for the events used in this analysis are shown in Appendix B.

D. Test Equipment

The physical characteristics for the scale models are shown in Table 2. The nominal Froude values are also shown. The moment of inertia values calculated for the scale model are considerably higher than the correct nominal Froude values.

Table 2. Scale Model Physical Properties

	M260	Scale Launcher	Froude Nominal Values
Weight (lbs)	35.000	4.375	4.375
CG (in)	34.325	17.163	17.163
Ixx (slug-ft ²)	0.123	0.006	0.004
Iyy (slug-ft ²)	2.630	0.128	0.082
Izz (slug-ft ²)	2.640	0.128	0.082
Length (in)	66.190	33.100	33.095
Diameter (in)	9.755	4.875	4.878

The ejector rack force was a constant value of 187 lbf with a travel of 1 inch. This value was scaled from the maximum force value of the Apache rack, used on the AH-64 helicopter, because this scale ejector rack was originally designed for a different test. This value is considerably higher than the correct scale values for the Talley Rack, used on the OH-58D, which was used in the full-scale events shown in this report. A comparison of the scale model ejector rack force with the correct scaled ejector force is shown in Figure 1.

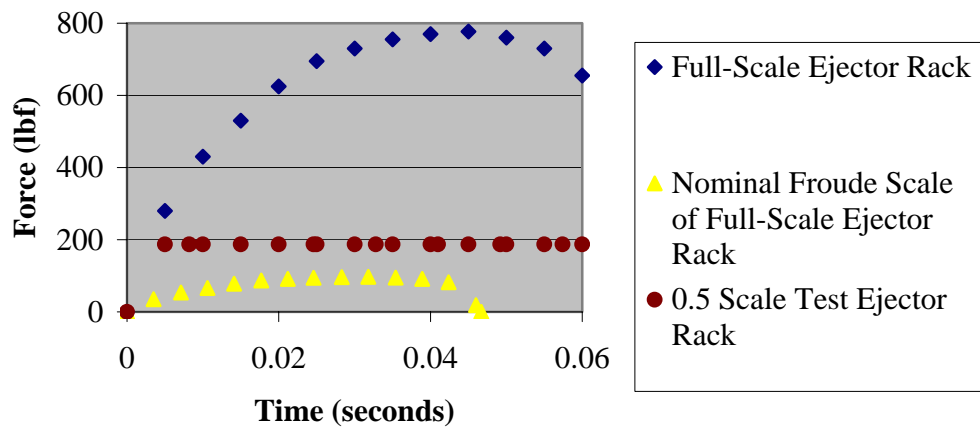


Figure 1. Comparison of Scale Ejector Force Versus Froude Nominal Values

The scale models and ejector rack were installed as shown in Figure 2.



Figure 2. Scale Model and Ejector Rack Installation

The ASVS camera and store jettison were controlled from the cockpit. The installation of the ASVS control box is shown in Figure 3.



Figure 3. ASVS Control Installation

An Inter-Range Image Generator (IRIG) was used to provide a timestamp to the film and digital images. The IRIG and ASVS data storage system were installed as shown in Figure 4.



Figure 4. IRIG Installation

III. ANALYSIS

A. Froude Scaling

The goal of aerodynamic scaling in wind tunnel applications can be accomplished if two criteria are met. These are (1) aerodynamic forces and moments on the model are directly scaleable to the real item; and (2) the inertial response of the model to applied forces and moments are directly scaleable to the real item. Aerodynamic scaling in wind tunnel applications is accomplished by exactly reducing the linear dimensions of the model by some scaling factor (1/2, 1/8, etc). The scale model is oriented in the wind tunnel in the same manner as the real object. If the velocity (Mach number) and Reynolds number are the same as the real item, then the aerodynamic forces and moments on the model will be directly scaleable to the real item.

The second goal is to be able to directly scale the observed motion of the scale model to the real item. In practice, it is often not possible to match both the Mach number and the Reynolds number for a given flight condition. Compromise scaling laws are required to obtain a workable solution.

Froude scaling is a compromise scaling law commonly used in wind tunnel testing for low-speed applications. This scaling maintains the ability to directly scale the dynamic motion of the scale model by sacrificing the requirement to match the Mach number and Reynolds number. This law is most accurate at low speeds where compressibility effects are small [2].

The Froude scaling relations used in this analysis are listed below. The prime denotes the scale model [3].

TIME

$$t' = t \times \sqrt{\Lambda}$$

VELOCITY

WEIGHT

$$V_{\infty}' = V_{\infty} \times \sqrt{\Lambda}$$
$$WT' = WT \times \left(\frac{\rho_{\infty}'}{\rho_{\infty}} \right) \times \Lambda^3$$

EJECTION FORCE

$$F_{E1}' = F_{E1} \times \left(\frac{\rho_{\infty}'}{\rho_{\infty}} \right) \times \Lambda^3$$

MOMENT OF INERTIA

$$I_{YY}' = I_{YY} \times \left(\frac{\rho_{\infty}'}{\rho_{\infty}} \right) \times \Lambda^5$$

where lambda (Λ) is the scale factor. In this analysis $\Lambda = 1/2$. The air density is denoted by ρ_{∞} . For this analysis, the ratio of the air densities between the scale model test and the full-scale test is equal to one.

If these relationships are observed in the construction of the model test conditions, then the dynamic motion properties of the model can be related to those of the real object by the following relations:

LINEAR TRANSLATIONS

$$Z' = Z \times \Lambda$$

ANGULAR MOTION

$$\theta' = \theta.$$

These relationships are used to directly compare the motion distances and rotation angles of the two tests.

B. Comparison

Scale model flight test data and full-scale flight test data can be compared in two ways. The first method is to directly compare the 6-DOF results of the two trajectories. This analysis will show results of these comparisons for the vertical motion (Z-axis, “down”) and pitch components. The second method is to compare the minimum miss-distance calculated based upon these two trajectories. The flight conditions selected for comparison are listed in Table 3. By selecting only flight conditions greater than 30 knots, the potential effect of rotor downwash is minimized.

Table 3. Comparison Flight Conditions

Test Point	Full-Scale Velocity (kts)	Half-Scale Velocity (kts)	Nominal Froude Scale Velocity (kts)
4	40	30	28.3
6	70	50	49.5
7	100	70	70.7

An example graph of a comparison in the vertical (“Z”) direction is shown in Figure 5. Comparisons for the 70 knots full-scale condition and the 100 knots full-scale condition are shown in Appendix C.

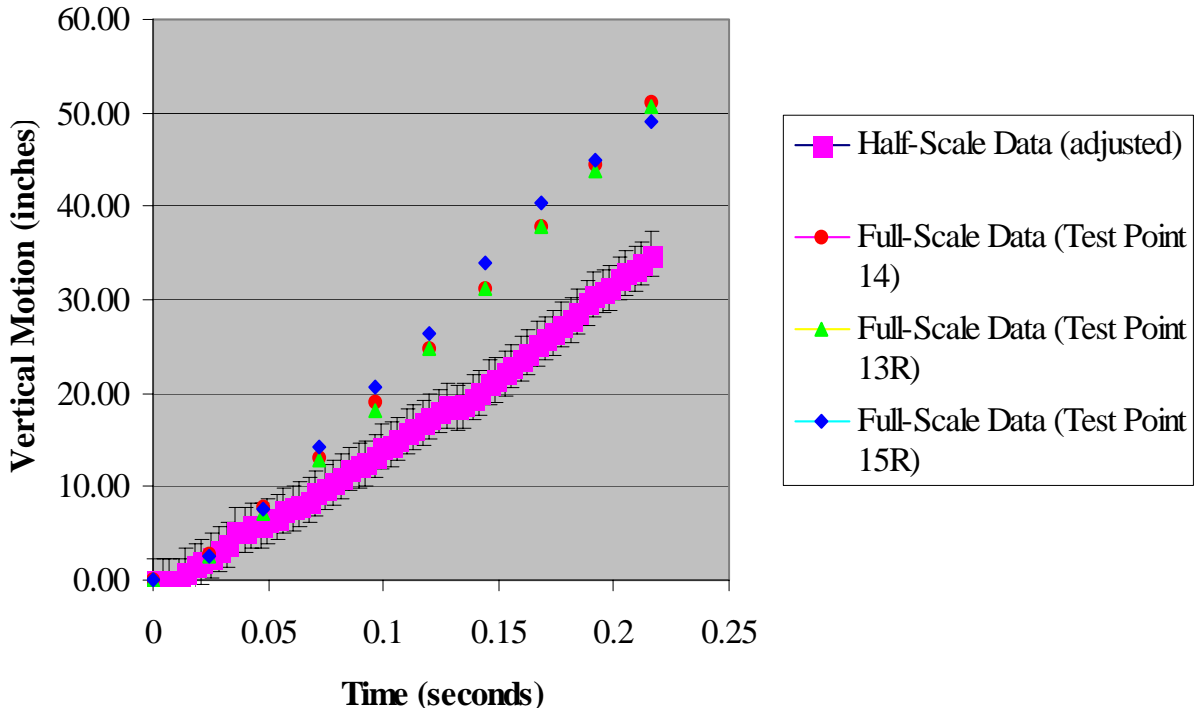


Figure 5. Comparison of Vertical Motion at 40 Knots Full-Scale Conditions

Figure 5 shows that the vertical motion is slightly under-predicted by the scale model test. The motion is generally linear, similar to the full-scale events, with a smaller slope. The full-scale events have good repeatability that provides confidence in these results.

An example graph of a comparison in the pitch rotation axis is shown in Figure 6. Comparison of other available conditions are compiled in Appendix D.

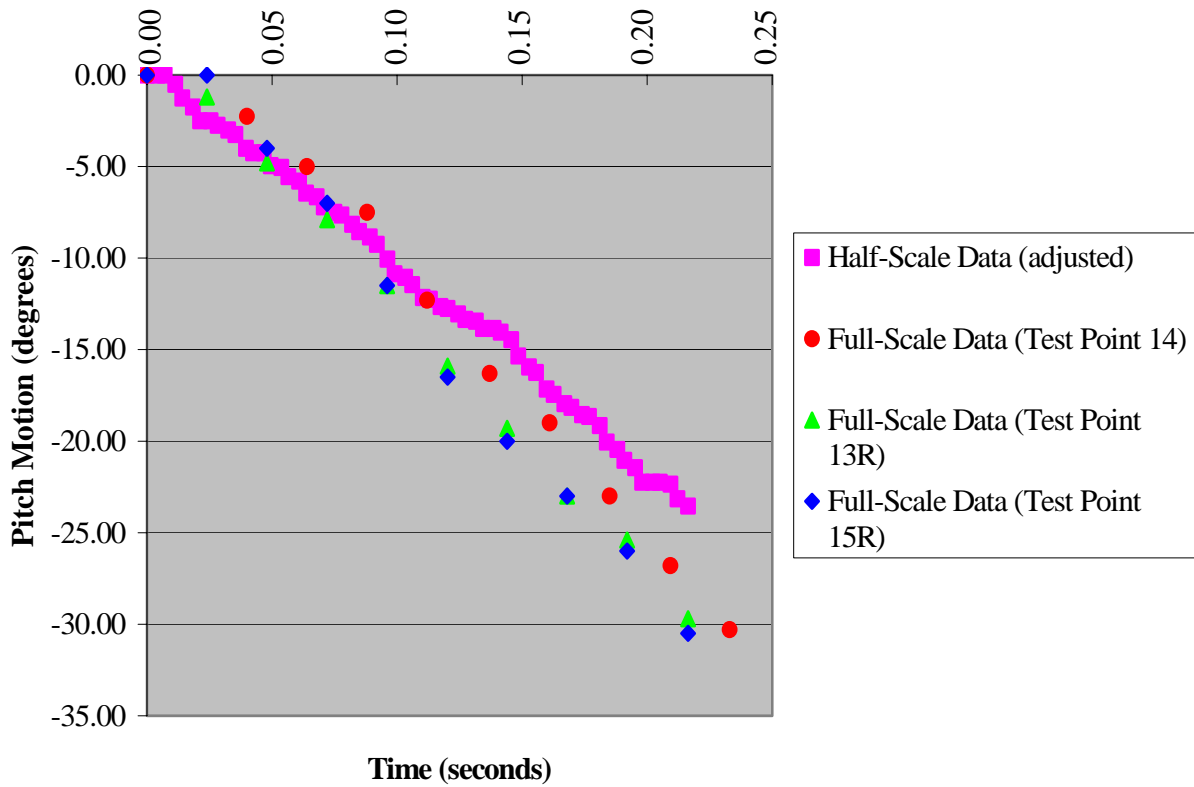


Figure 6. Comparison of Pitch Axis Motion at 40 Knots Full-Scale Conditions

Figure 6 shows that the pitch motion is slightly under-predicted by the scale model test. The motion is linear, similar to the full-scale tests, with a smaller slope. The full-scale events have good repeatability, which provides confidence in these results.

An example graph with a comparison of miss-distance versus time using the full-scale trajectory and the scaled data is shown in Figure 7. Comparisons for all selected conditions are compiled in Appendix E.

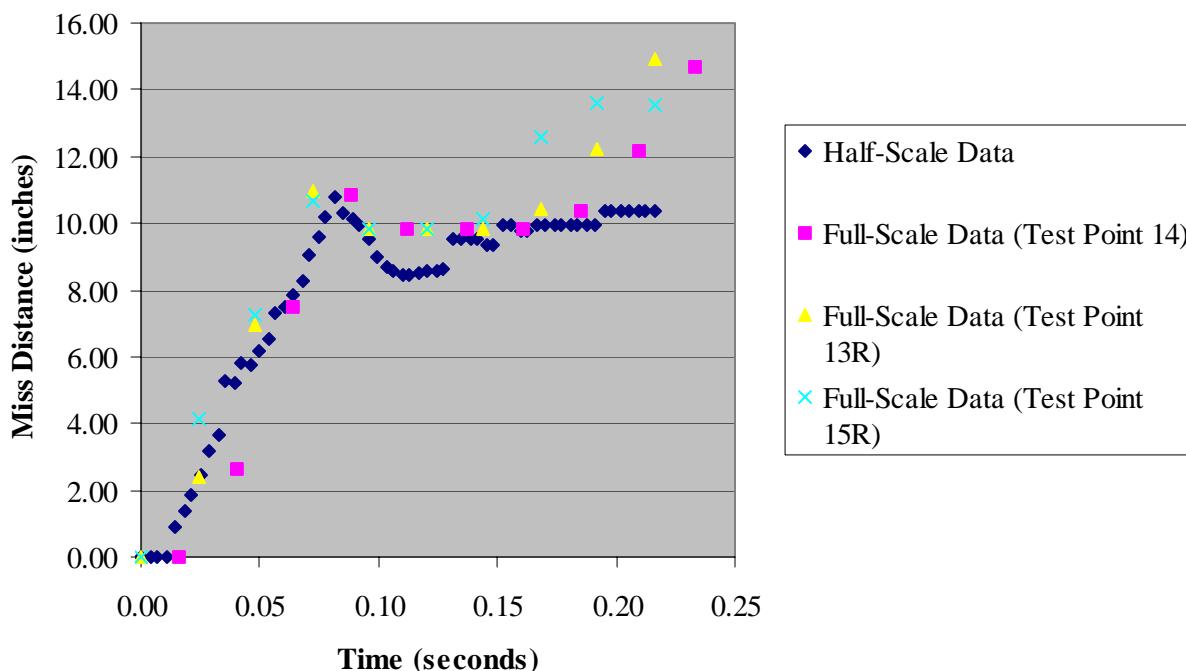


Figure 7. Calculated Miss-Distance Versus Time Curves at 40 Knots Full-Scale Conditions

Figure 7 shows good agreement between the scale model event and the full-scale event. The full-scale events show good repeatability, which provides confidence in these results.

C. Discussion

In all cases, the vertical motion is under-predicted by the scale model test. This is an unexpected result since the ejector force used is considerably higher than the correct Froude scale value. The slope is linear, similar to the full-scale tests, but smaller.

In all cases, the pitch motion is under-predicted by the scale model test. This is an expected result since the calculated moment of inertia values of the scale model are considerably higher than the nominal Froude scale values. However, the ejector force is considerably higher than the nominal Froude scale value, which should tend to counteract this effect.

In the 40 knots and 100 knots case, the miss-distance versus time calculation shows good agreement between the half-scale event and the full-scale event. In the 70 knots case, the agreement is not good (Fig. E-1). This is because the yaw motion in this particular trajectory is much larger than those in other events (Tables B-2 and B-3). This is the only case that exhibits a relatively large yaw motion. The full-scale events show minimal yaw motion with good agreement, which provides confidence that the yaw motion seen in the half-scale event is not a typical result. However, without a larger, statistically significant number of repeat tests, it is not possible to determine this for certain.

D. Error Sources

The ejector force for the scale model events was not correctly scaled to correspond to the force of the Talley rack, which is used on the OH-58D helicopter. The force was significantly larger than the theoretical scale values, but for a shorter time.

The mass moment of inertia values of the scale models were significantly larger than the theoretical scale values as shown in Table 2. This is the most likely explanation for the under-prediction of the pitch axis motion. The pitch axis motion is directly proportional to the ejector force and inversely proportional to the mass moment of inertia. It is unclear if the mass moment of inertia or the ejector force has a larger effect on pitch motion.

The scale model stores had lugs that were significantly larger than what would be appropriate for a strict Froude scale model. This was due to mechanical interface considerations. The lugs were constructed to enable the stores to connect to the ejector and have sufficient strength to be carried and jettisoned.

Because different helicopters were used in the full-scale test and the half-scale test, it is reasonable to expect the differences in rotor downwash to have an effect on the results. The higher speed test cases were selected for comparison because the rotor downwash for these cases should not be a factor. However, even in a strong rotor downwash, it is possible that there is not a large effect. In order to determine if this is the case, an analysis was conducted using simulation. An example case was calculated using the data for the half-scale test at 40 knots full-scale conditions, which should be the worst case. The downwash was modeled as hover downwash. The simulation was also run without downwash. The results are shown in Appendix F. Figures F-1 and F-2 show that the effect of downwash on the store motion is minimal.

E. Error Analysis

In order to determine which variable has a greater effect on the scale model test results, simulation was used to analyze trends. The baseline configuration of the scale model tests was simulated as conducted. Each of the likely error sources was then adjusted to the theoretically correct values and the simulation run again. The trends resulting from these changes were then applied to the original test data to estimate what the results would be if the scale model tests had been conducted with correct scaling. Since downwash was shown to be a non-factor in the preliminary analysis, these simulations were conducted without downwash to eliminate another variable.

The Trajectory Generation Program (TGP) is a Government-owned code developed at the Arnold Engineering Development Center (AEDC) to simulate the separation of objects from helicopters during flight. This code was used to simulate the scale model tests.

Missile DATCOM is a government-owned code developed at Wright-Patterson Air Force Base to estimate the aerodynamic force and moment coefficients of missiles. This code was used to calculate the change in aerodynamic force and moment coefficients resulting from the incorrect scaling of the lugs.

Figure 8 shows the baseline scale model configuration results for vertical motion at 40 knots full-scale conditions.

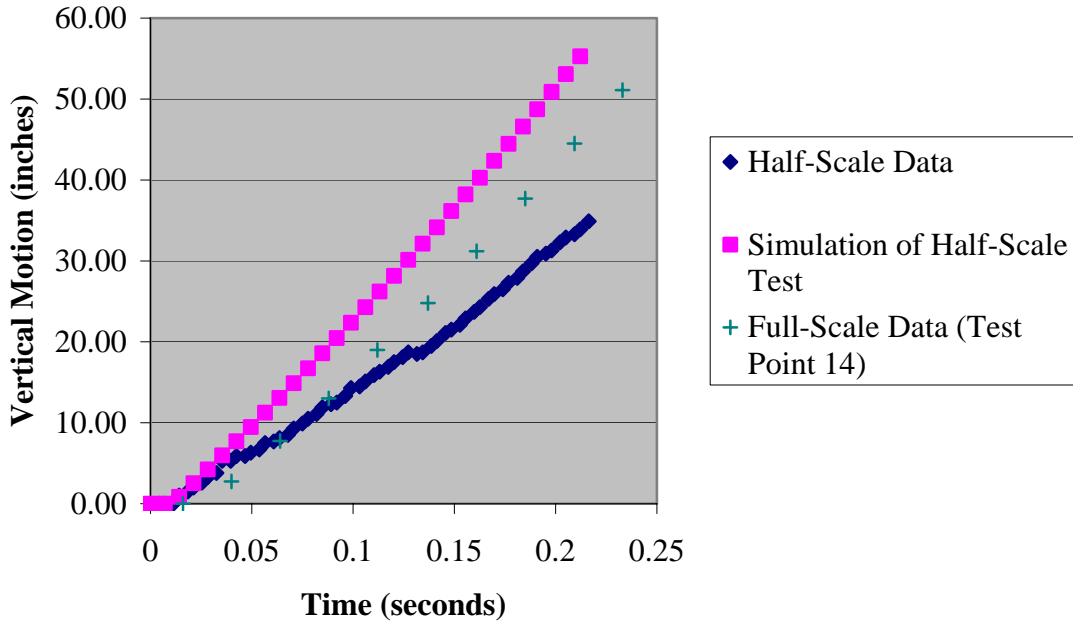


Figure 8. Simulation of Half-Scale Test, Vertical Motion, 40 Knots Full-Scale

Figure 9 shows the baseline scale model configuration results for pitch motion at 40 knots full-scale conditions.

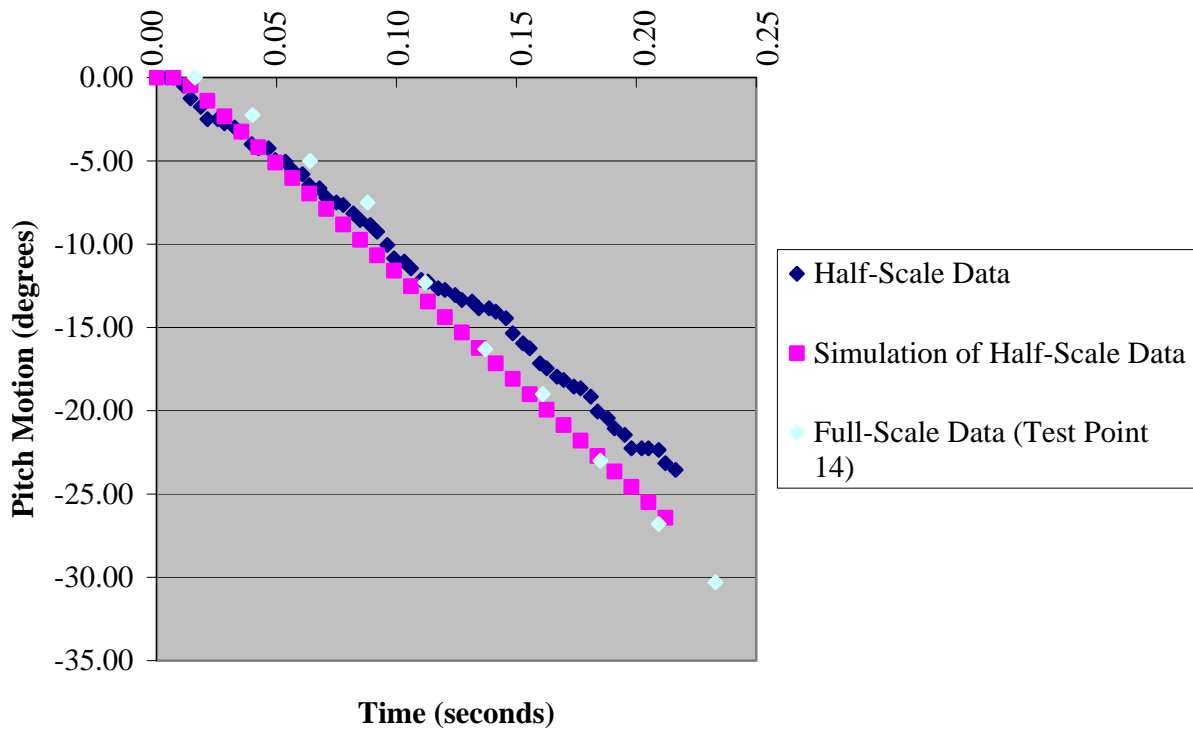


Figure 9. Simulation of Half-Scale Test, Pitch Motion, 40 Knots Full-Scale

Baseline results for the 70 knots full-scale condition and the 100 knots full-scale condition are shown in Appendix G. Similar to Figures 8 and 9, the vertical motion is over-predicted and the pitch motion is under-predicted.

Despite discrepancies with the vertical motion test data, the simulation results can still demonstrate trends, which are introduced by correcting the scaling errors of the half-scale test. Figure 10 shows the effect of using the correct mass moments of inertia on the vertical motion at the 40 knots full-scale condition.

Figure 10 shows that mass moment of inertia has little effect on the vertical motion. This is the expected result. Results are similar at 70 knots and 100 knots conditions. Figure 11 shows the effect of mass moment of inertia on the pitch motion at 40 knots full-scale conditions.

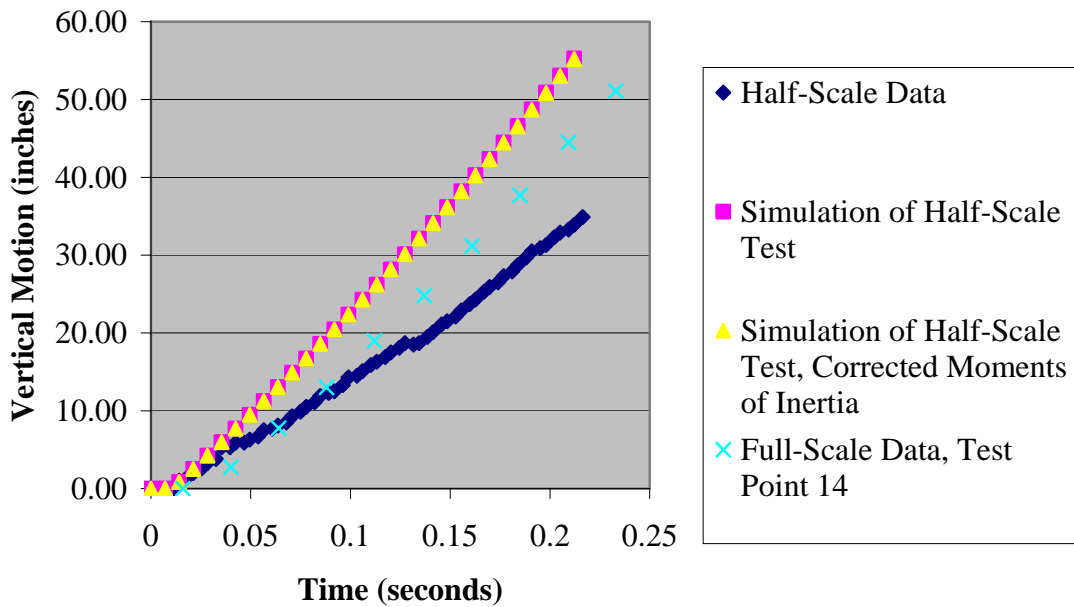


Figure 10. Effect of Mass Moment of Inertia on Vertical Motion, 40 Knots Full-Scale Conditions

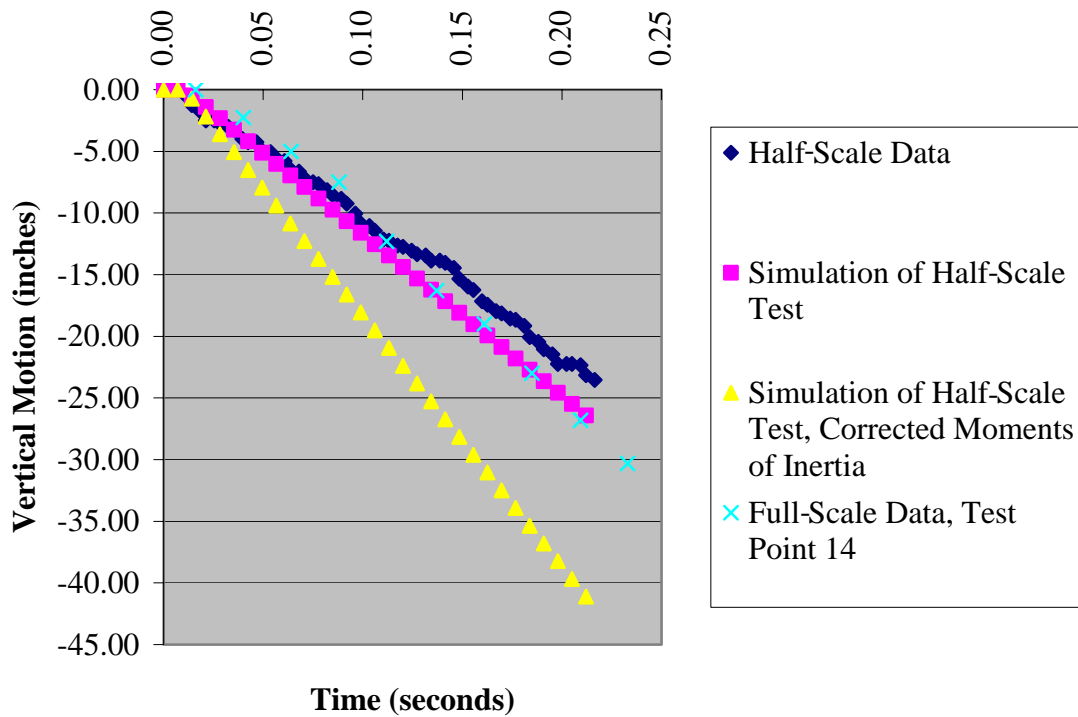


Figure 11. Effect of Mass Moment of Inertia on Pitch Motion, 40 Knots Full-Scale Conditions

Figure 11 shows that mass moment of inertia has a pronounced effect on pitch motion. This is the expected result. Results at 70 knots and 100 knots full-scale conditions are similar.

Figure 12 shows the effect of using the correctly scaled ejector forces on the vertical motion at 40 knots full-scale conditions.

Figure 12 shows the ejector forces have a pronounced effect on the vertical motion. This is the expected result. The simulation shows that the vertical motion starts with a gentler slope, but ends with a larger slope. This is because the correctly scaled ejector forces are less, but the store stays connected to the ejector rack longer, so the total impulse imparted to the separating store is larger. Figure 13 shows the effect of ejector forces on the pitch motion.

Figure 13 shows that ejector force has approximately the same effect on pitch motion as it does on vertical motion. The effect of ejector force on vertical motion and pitch motion at 70 knots and 100 knots full-scale conditions is similar to Figures 12 and 13, respectively.

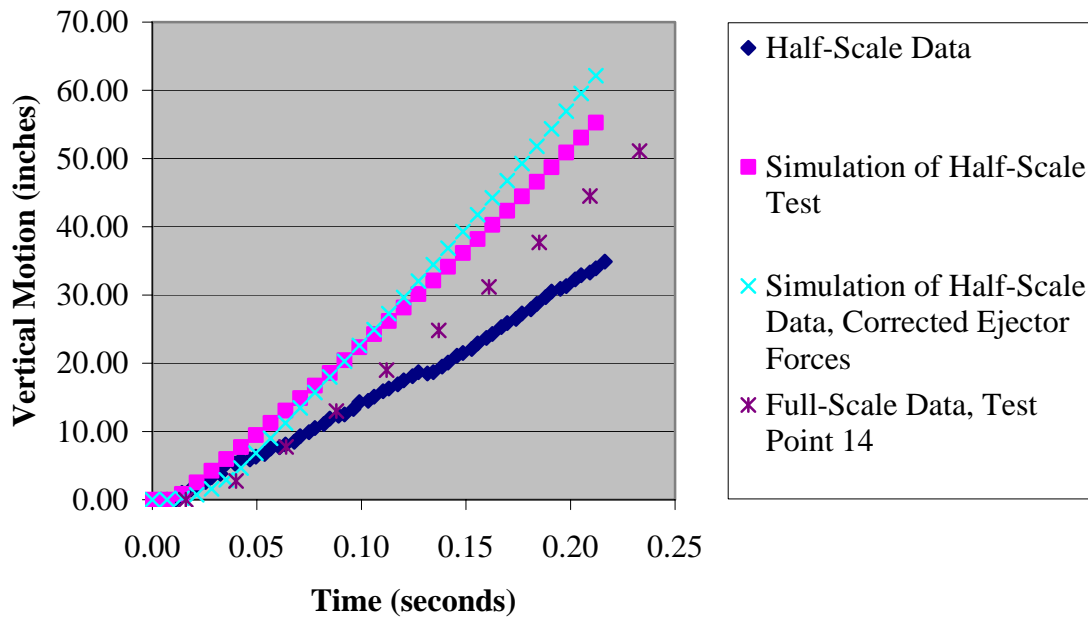


Figure 12. Effect of Ejector Force on Vertical Motion, 40 Knots Full-Scale Conditions

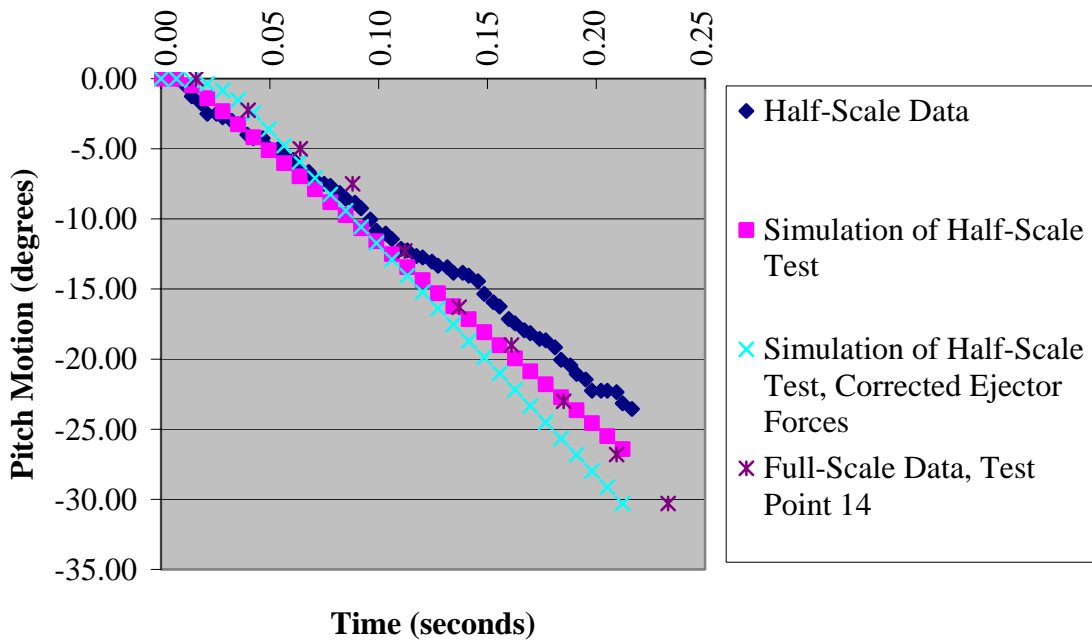


Figure 13. Effect of Ejector Force on Pitch Motion, 40 Knots Full-Scale Conditions

Figure 14 shows the effect of properly scaled lugs on vertical motion at 40 knots full-scale conditions.

Figure 14 shows that lug size has a negligible effect on vertical motion. Review of the coefficients supplied by DATCOM shows that the smaller lugs result in a smaller axial force coefficient, but a negligible change in other coefficients. Figure 15 shows the effect of lug size on pitch motion.

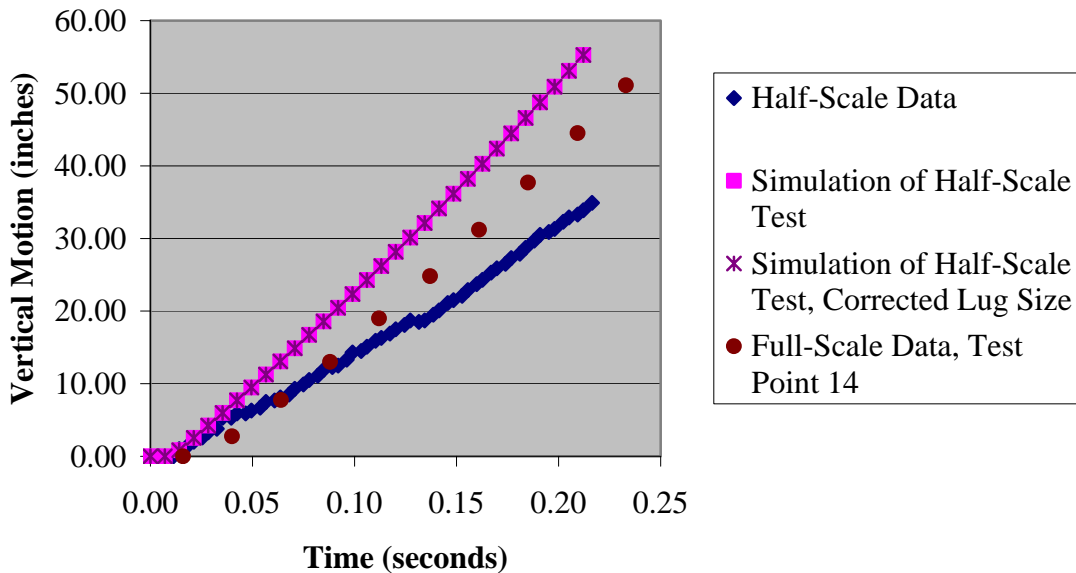


Figure 14. Effect of Lug Size on Vertical Motion, 40 Knots Full-Scale Conditions

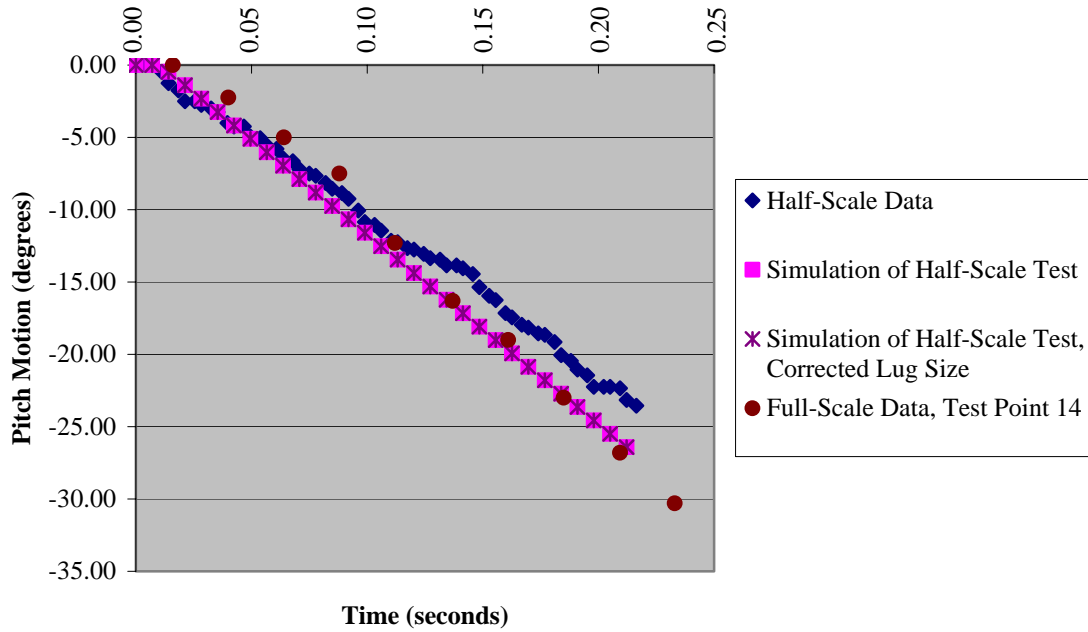


Figure 15. Effect of Lug Size on Pitch Motion, 40 Knots Full-Scale Conditions

Figure 15 shows that lug size has a negligible effect on pitch motion. The results for vertical motion and pitch motion at 70 knots and 100 knots full-scale conditions are similar to Figures 14 and 15, respectively.

Figures 10 through 15 show that the two major variables controlling the vertical motion and pitch motion slopes are the mass moment of inertia and the ejector force. Another simulation was conducted to estimate the effect of correctly scaling both of these variables. Figure 16 shows the effect of correctly scaling both of these variable on the vertical motion at 40 knots full-scale conditions.

Figure 16 shows that correctly scaling both variables have the same effect on vertical motion as correct scaling of the ejector forces. Results for 70 knots and 100 knots full-scale conditions are similar. These results are shown in Appendix H. Figure 17 shows the effect of correctly scaling both of these variables on the pitch motion at 40 knots full-scale conditions.

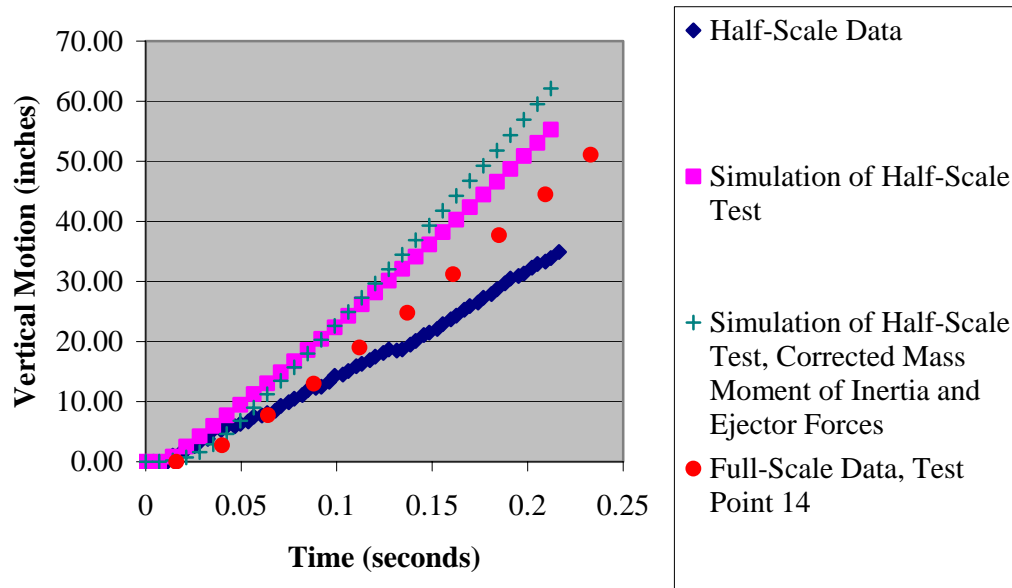


Figure 16. Effect of Mass Moment of Inertia and Ejector Forces on Vertical Motion, 40 Knots Full-Scale Conditions

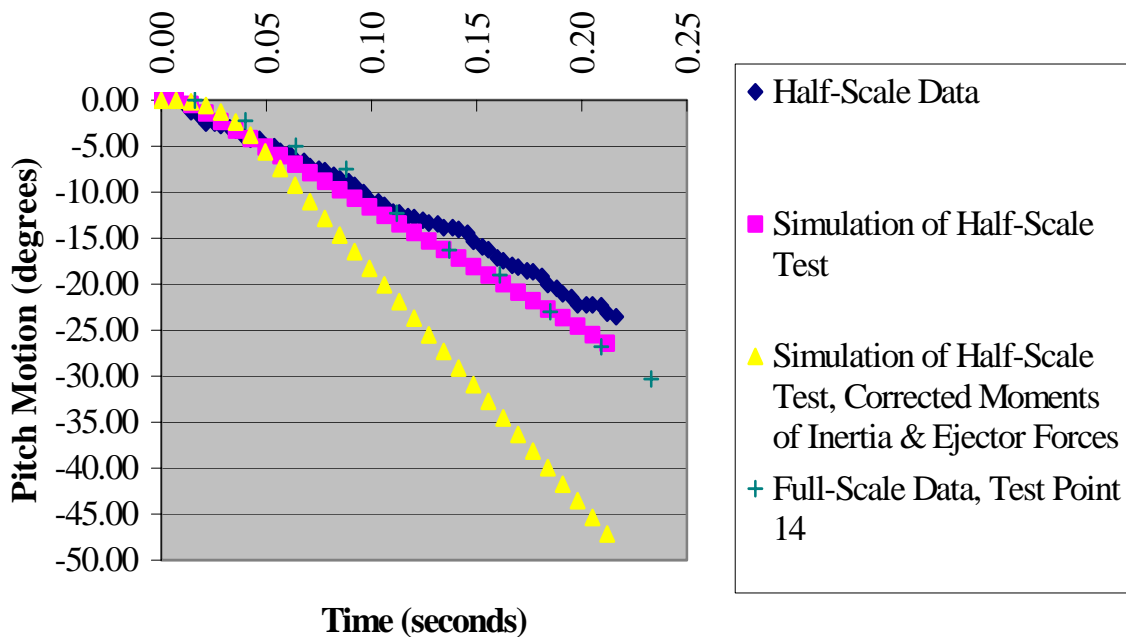


Figure 17. Effect of Mass Moment of Inertia and Ejector Forces on Pitch Motion, 40 Knots Full-Scale Conditions

Figure 17 shows that the effect of correctly scaling these two variables has an additive effect on the pitch motion. This is the expected result, based upon Figures 11 and 13. The results for 70 knots and 100 knots full-scale conditions are similar. These results are shown in Appendix H.

F. Error Correction

The effect of Figures 16 and 17 on the actual half-scale data was estimated by adjusting the slope of the vertical and pitch motion curves by the change in slope found between the simulation results. A least squares fit was calculated for each curve slope. This equation was adjusted by the ratio of the slopes from the simulations for the half-scale test and the half-scale test with corrected ejector forces and mass moments of inertia. This adjusted slope was then used to calculate a new trajectory. Figure 18 shows the results of applying the effects of correctly scaling the mass moment of inertia and ejector forces for the vertical motion at 40 knots full-scale conditions.

Figure 18 shows that adjusting the trajectory curve for correct scaling of mass moment of inertia and ejector forces results in a vertical motion curve with a slightly higher slope. This provides a small amount of improvement in the correlation with full-scale data. The results for 70 knots and 100 knots full-scale conditions are similar. These results are shown in Appendix I. Figure 19 shows the effect of the mass moment of inertia and ejector forces on the pitch motion of the half-scale data at 40 knots full-scale conditions.

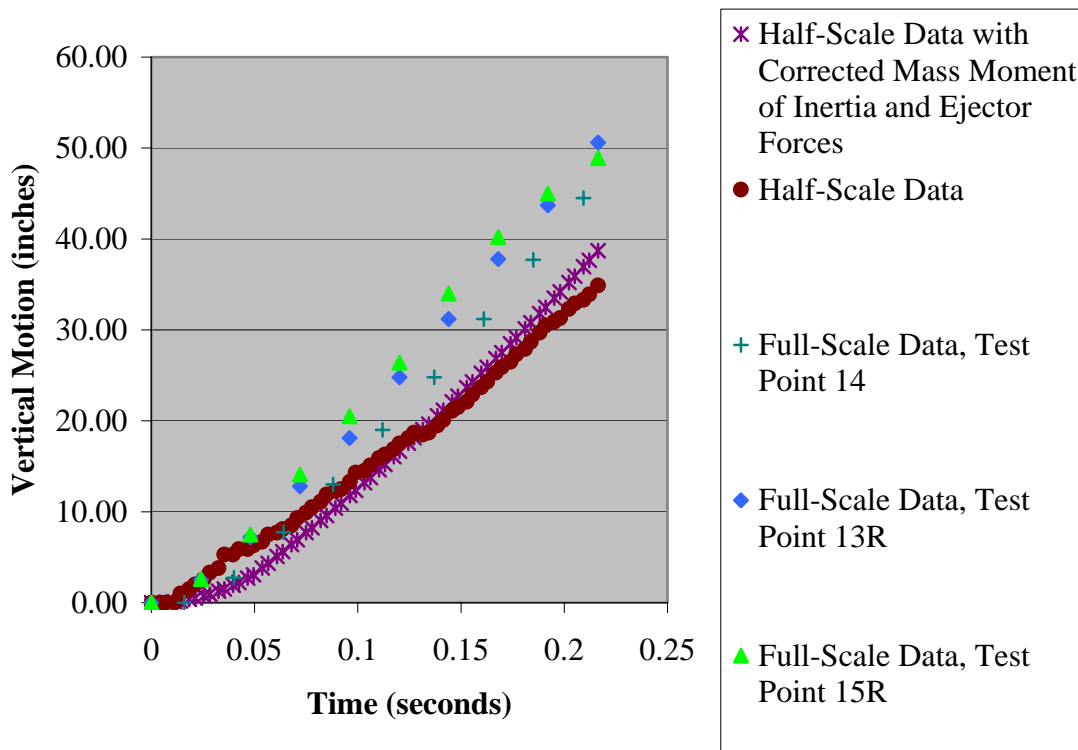


Figure 18. Effect of Ejector Forces and Mass Moment of Inertia on Half-Scale Vertical Motion Data, 40 Knots Full-Scale Conditions

Figure 19 shows a large change in the pitch motion slope. The resulting trajectory has worse correlation with full-scale data because the half-scale data already has strong correlation. Figure 20 shows the effect of the mass moment of inertia and ejector forces on the pitch motion of the half-scale data at 70 knots full-scale conditions.

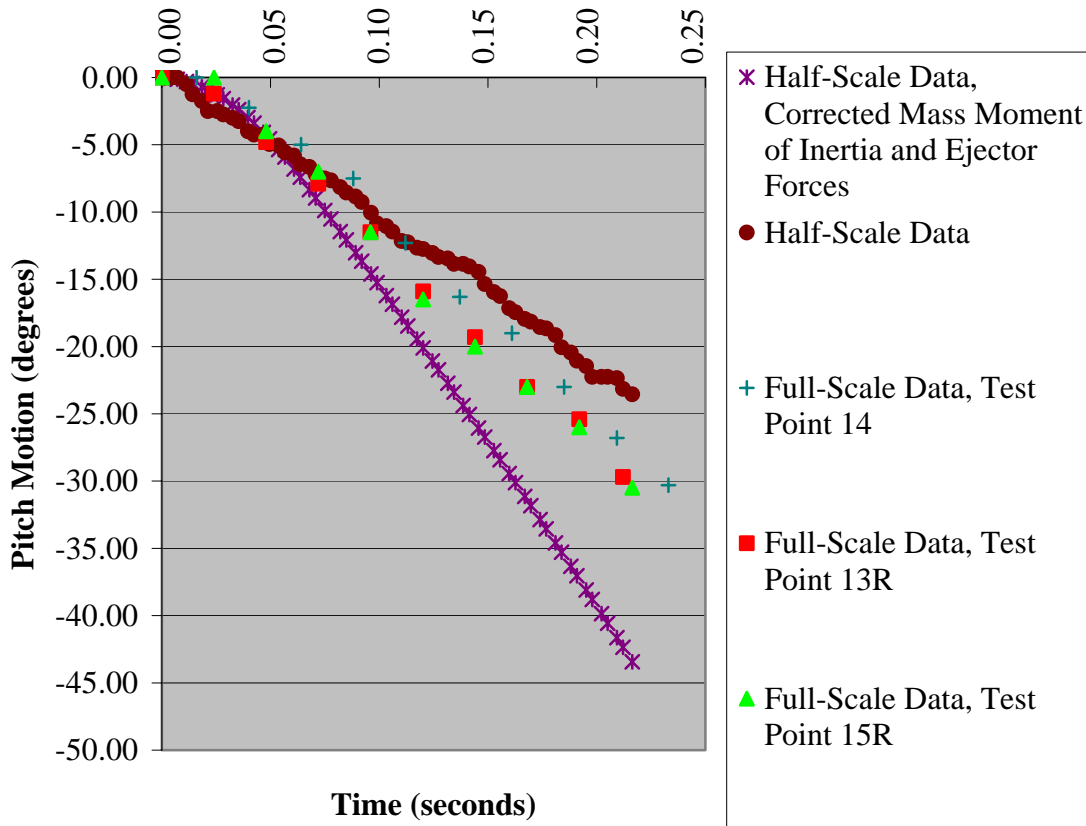


Figure 19. Effect of Ejector Forces and Mass Moment of Inertia on Half-Scale Pitch Motion Data, 40 Knots Full-Scale Conditions

Figure 20 shows a large change in the pitch motion slope. The resulting trajectory has excellent correlation with full-scale data. Figure 21 shows the effect of the mass moment of inertia and ejector forces on the pitch motion of the half-scale data at 100 knots full-scale conditions.

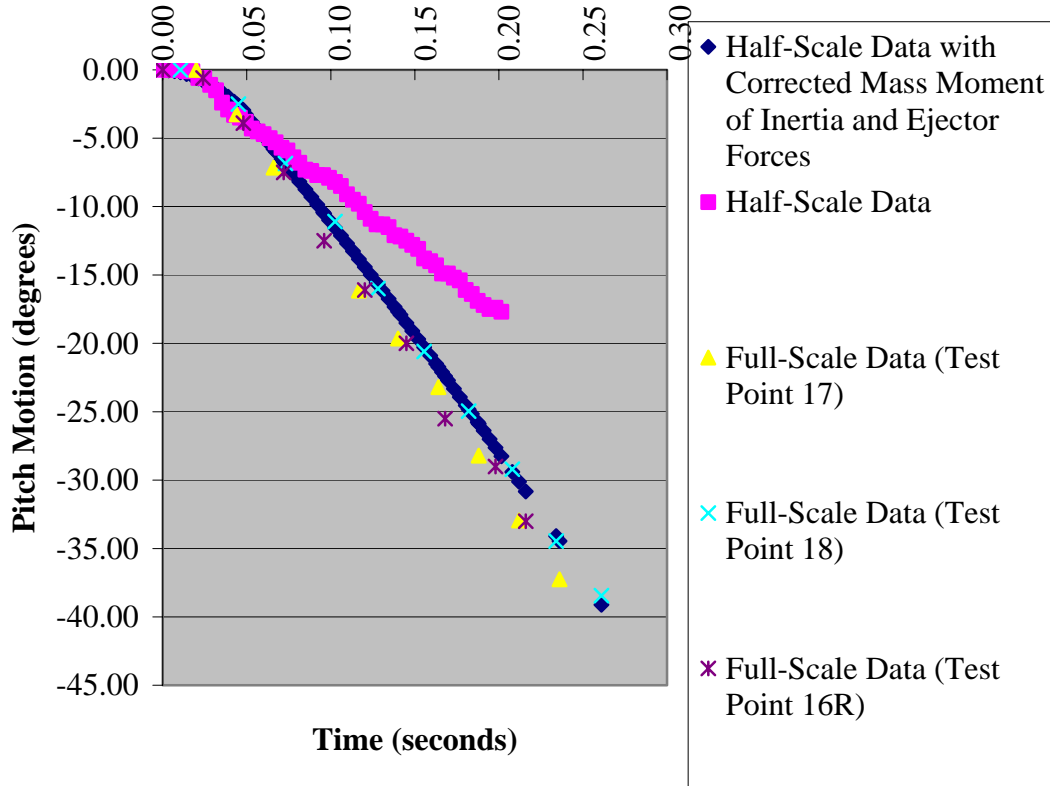


Figure 20. Effect of Ejector Forces and Mass Moment of Inertia on Half-Scale Pitch Motion Data, 70 Knots Full-Scale Conditions

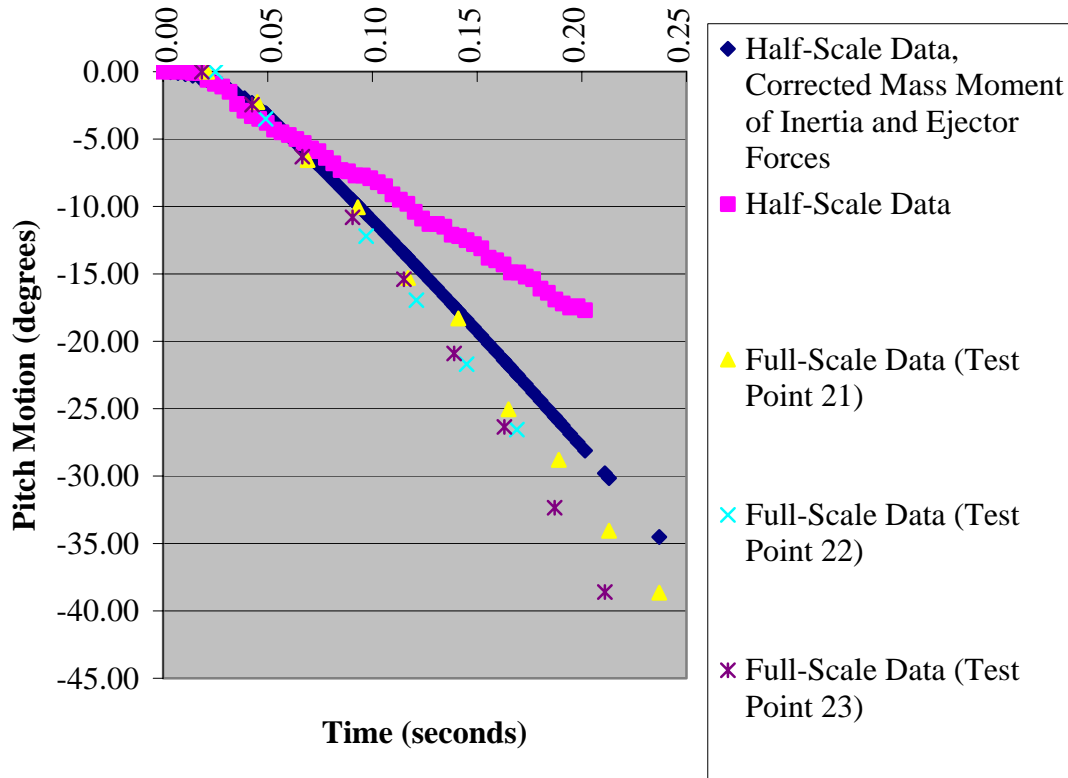


Figure 21. Effect of Ejector Forces and Mass Moment of Inertia on Half-Scale Pitch Motion Data, 100 Knots Full-Scale Conditions

Figure 21 shows a large change in the pitch motion slope. The resulting trajectory has improved correlation with full-scale data. Figures 20 and 21 show that correctly scaling the mass moment of inertia and ejector forces should increase the correlation with full-scale data for vertical motion at all speeds tested and increase correlation for pitch motion at the higher velocities.

Although the pitch motion correlation decreases at the lower velocity, this may not result in a worse miss-distance estimate. In order to determine the effect of these variables on miss-distance, the corrected vertical motion from Figure 18 and the pitch motion from Figure 19 were added to the other 4-DOF from the original half-scale data. This estimated trajectory was run through the CLRANC code to obtain an estimated miss-distance versus time function. Figure 22 shows the results of this calculation.

Figure 22 shows that correcting the trajectory of the half-scale test for the effects of mass moment of inertia and ejector forces results in improved correlation with test data early in the trajectory and the same correlation as the uncorrected half-scale test data in the later part of the trajectory, including the closest approach to the helicopter. This means that correcting half-scale data using trends developed through simulation results in the same miss-distance estimate or better. This result can be considered worst case because the trajectory correlation at higher velocities is better than this example.

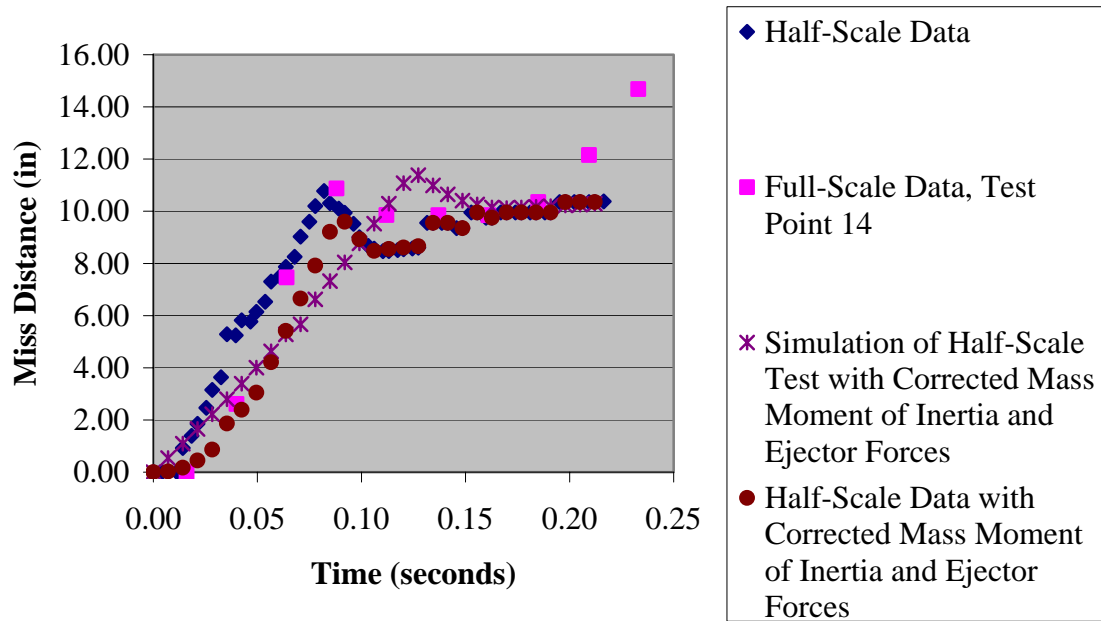


Figure 22. Effect of Mass Moment of Inertia and Ejector Forces on Miss-Distance at 40 Knots Full-Scale Conditions

IV. CONCLUSIONS AND RECOMMENDATIONS

A. Conclusions

The objective of this effort was to compare the calculated trajectories of jettison events from two tests to determine the feasibility of using scale models and non-military helicopters to collect test data instead of using real external stores on military helicopters. The conclusions may be summarized as follows:

1. Both the vertical motion and pitch motion encountered in the scale model testing under-predict those of the full-scale event.

2. Statistically significant numbers of scale model tests are required to be conducted at the same nominal conditions in order to enable a thorough uncertainty analysis of the resulting trajectories.

3. For ejector-dominated separation events, correct scaling of the mass moments of inertia is crucial to accurately modeling the angular motions of full-scale events using scale models. Mass moment of inertia values have a dramatic impact on the trajectory pitch motion.

4. For ejector-dominated separation events, correct scaling of the ejector forces is crucial to accurately modeling the angular motions and vertical motions of full-scale events using scale models. Ejector forces have a noticeable affect on both the vertical motion and pitch motion.

5. Correct scaling of protuberances such as ejector lugs is relatively unimportant for accurately modeling the angular motions and vertical motions of full-scale events using scale models.

6. Based upon the limited test data available, the vertical motion predicted using the scale model testing is not close to the vertical motion of full-scale test data. However, for ejector-dominated events at minimum sideslip, the under-prediction of the vertical motion does not strongly affect the value of the calculated miss-distance. For separation events at these conditions, scale model testing on non-military helicopters can produce useable results.

7. Simulation shows that the rotor downwash does not significantly affect the trajectory of ejector-dominated separation events at minimum sideslip conditions.

8. Adjusting scale model test data based upon simulation trends can improve correlation to full-scale for test data with errors in model construction. In this effort, the estimated effect of errors in mass moment of inertia and ejector forces were corrected. Correlation of the vertical motion was improved at all velocity conditions. Correlation of the pitch motion was improved at higher velocities, but decreased at the lowest velocity condition studied.

B. Recommendations

Based upon the conclusions of the previous section, the following recommendations have been developed:

1. Additional scale model testing is recommended. Statistically significant numbers of tests should be conducted at the same nominal conditions. This will enable a thorough uncertainty analysis of the resulting trajectories.

2. For ejector-dominated separation events at minimum sideslip, miss-distance calculations using scale data is close to the miss-distance calculated for full-scale events at lower velocities (approximately 0 to 40 knots) and at higher velocities (approximately 80 knots and above). Results at these conditions should be used to predict store miss-distances. Additional testing is recommended to determine if miss-distance calculations can be trusted at intermediate velocities.

3. Recommend adjusting scale model test data based upon simulation trends to correct for inaccuracies in the modeling process for intermediate to high-test velocities (approximately 50 knots and higher).

REFERENCES

1. Robinson, C.E., "Validation of a Simulation Technique for Predicting and Visualizing Helicopter Store Separation Trajectories", AEDC-TMR-95-P23, Sverdrup Technology Inc., January 1996.
2. Keen, K.S.; Morgret, C.H., and Artebury; R.L., "An Analytic Investigation of Accuracy Requirements for Onboard Instrumentation for Dynamically-Scaled Wind Tunnel Drop Models", Memorandum for Record, Calspan/AEDC Operations, June 1993, pp 40-41.
3. Wolowicz, Chester H.; Bowman, James S. Jr.; and Gilbert, William P., "Similitude Requirements and Scaling Relationships as Applied to Model Testing", NASA TP-1435, August 1979.

ABBREVIATIONS

2-DOF	Two Degree-of-Freedom
6-DOF	Six Degree-of-Freedom
AED	Aviation Engineering Directorate
AEDC	Arnold Engineering Development Center
ASVS	Airborne Separation Video System
CASSAS	Computer-Aided Store Separation Analysis System
CG	Center of Gravity
CLRANC	Clearance and Collision Detection Code
deg	Degrees
DOD	Department of Defense
DOF	Degrees of Freedom
ft	Feet
in	Inches
IRIG	Inter-Range Image Generator
Ixx	Mass Moment of Inertia about the roll axis
Iyy	Mass Moment of Inertia about the pitch axis
Izz	Mass Moment of Inertia about the yaw axis
kts	Knots
lbs	Pounds
RWSI	Rotary Wing Stores Integration
SEO	Seek Eagle Office
SGAP	Store-Separation Graphic Analysis Package
TGP	Trajectory Generation Program
WMASC	Weapons Modification and Simulation Capability
YPG	U.S. Army Yuma Proving Ground

LIST OF SYMBOLS

F_{E1}	Ejection Force
F_{E1}'	Scale Model Ejection Force
I_{YY}	Pitch Axis Mass Moment of Inertia
I_{YY}'	Scale Model Pitch Axis Mass Moment of Inertia
t	Time
t'	Scale Model Time
V_{∞}	Free Stream Velocity
V_{∞}'	Scale Model Free Stream Velocity
WT	Store Weight
WT'	Scale Model Weight
Z	Store Vertical Motion
Z'	Scale Model Vertical Motion
Θ	Store Pitch Motion
Θ'	Scale Model Pitch Motion
Λ	Scaling Ratio
ρ_{∞}	Free Stream Air Density
ρ_{∞}'	Scale Model Free Stream Air Density

APPENDIX A
TRAJECTORY DATA TABLES

**APPENDIX A
TRAJECTORY DATA TABLES**

**Table A-1
OH-58D Jettison Test Matrix**

**Measured Aircraft Flight Conditions
At Store Release**

Series	Test Pt	Flight Cond	Store	U kts	V kts	W kts
rws_i_01	tp01	hover	Empty	0.78	-2.10	-0.12
rws_i_01	tp02	hover	Empty	-0.87	-0.83	-0.67
rws_i_01	tp03	hover	Empty			
rws_i_01	tp04	hover	2 dummies	-2.06	0.067	-0.18
rws_i_01	tp05	hover	2 dummies	0.11	-0.31	0.75
rws_i_01	tp06	hover	2 dummies	1.95	0.18	-1.29
rws_i_01	tp07	20kts	Empty	20.49	3.82	-1.20
rws_i_01	tp08	no data				
rws_i_01	tp09	no data				
rws_i_01	tp10	20kts	2 dummies	16.67	3.43	0.13
rws_i_01	tp11	20kts	2 dummies	19.29	3.17	0.55
rws_i_01	tp12	20kts	2 dummies	22.30	3.51	-0.03
rws_i_01	tp13	no data				
rws_i_01	tp14	40kts	Empty	29.67	5.49	-1.63
rws_i_01	tp15	no data				
rws_i_02	tp16	no data				
rws_i_02	tp17	70kts	Empty	76.30	14.82	1.59
rws_i_02	tp18	70kts	Empty	70.98	13.24	-2.71
rws_i_02	tp19	no data				
rws_i_02	tp20	no data				
rws_i_02	tp21	100kts	Empty	98.95	17.87	2.27
rws_i_02	tp22	100kts	Empty	100.30	19.04	-1.22
rws_i_02	tp23	100kts	Empty	102.45	19.95	-0.94
rws_i_02	tp24	no data				
rws_i_02	tp25	100(1)	Empty	103.19	17.11	0.08
rws_i_02	tp26	100(1)	Empty	103.40	17.23	1.48
rws_i_02	tp27	100(2)	Empty	102.52	17.92	-1.20
rws_i_02	tp28	100(2)	Empty	102.19	21.35	-1.79
rws_i_02	tp29	100(1)	Empty	99.50	20.30	1.13

**Table A-1
OH-58D JETTISON TEST (Concluded)**

**Measured Aircraft Flight Conditions
At Store Release**

Series	Test pt	Flight Cond	Store	U kts	V kts	W kts
rws_i_02	tp30	70(3)	Empty	105.00	24.01	-0.27
rws_i_02	tp31	70(3)	Empty	76.31	14.85	-5.43
rws_i_02	tp32	70(3)	Empty	75.96	13.30	-4.16
rws_i_02	tp33	70(4)	Empty	74.42	13.97	-7.03
rws_i_02	tp34	70(4)	Empty	76.04	13.57	-13.94
rws_i_02	tp35	70(4)	Empty	74.50	14.15	-15.69
rws_i_02	tp36	15 side	Empty			
rws_i_02	tp37	15 side	Empty			
rws_i_02	tp38	15 side	Empty			
rws_i_02	tp39	no data	Empty	-7.28	-1.08	-8.59
rws_i_02	tp40	15 rear	Empty	-7.03	-1.05	-8.39
rws_i_02	tp41	15 rear	Empty	-3.32	-1.10	-1.30
rws_i_04	tp01r	hover	Empty			
rws_i_04	tp04r	hover	2	-1.30	1.89	0.67
			dummies			
rws_i_04	tp08r	20kts	Empty	-27.13	31.33	0.03
rws_i_04	tp09r	20kts	Empty	-14.84	24.76	-0.10
rws_i_04	tp10r	20kts	2	-22.43	24.99	3.33
			dummies			
rws_i_04	tp13r	40kts	Empty	-32.02	42.02	-1.76
rws_i_04	tp15r	40kts	empty	-26.85	41.98	-0.98
rws_i_04	tp16r	70kts	empty	43.55	63.23	-1.03
rws_i_04	tp24r	100kts	empty	-50.96	94.53	-1.93
rws_i_04	tp38r	15 side	empty	-11.15	-3.23	-0.65
rws_i_04	tp39r	15 rear	empty	1.91	-0.28	-0.76

Note: The store is a 7-tube rocket launcher, designated M260

- (1) 1 ball left
- (2) 1 ball right
- (3) 500 feet per minute descent
- (4) 1000 feet per minute descent

**Table A-2
Trajectory Data, OH-58D,
Test Point13R**

Time, Sec	x position, ft	y position, ft	z position, ft	psi, deg	yheta, deg	phi, deg
0.00E+00	0.00E+00	0.00E+00	0.00E+00	0.00E+00	0.00E+00	0.00E+00
2.40E-02	0.00E+00	0.00E+00	2.50E+00	0.00E+00	-1.20E+00	0.00E+00
4.80E-02	-1.00E-01	0.00E+00	7.20E+00	0.00E+00	-4.80E+00	0.00E+00
7.20E-02	3.00E-01	0.00E+00	1.28E+01	0.00E+00	-7.90E+00	0.00E+00
9.60E-02	5.00E-01	0.00E+00	1.81E+01	0.00E+00	-1.15E+01	0.00E+00
1.20E-01	8.00E-01	0.00E+00	2.48E+01	0.00E+00	-1.59E+01	0.00E+00
1.44E-01	8.00E-01	0.00E+00	3.12E+01	0.00E+00	-1.93E+01	0.00E+00
1.68E-01	-6.00E-01	0.00E+00	3.78E+01	0.00E+00	-2.30E+01	0.00E+00
1.92E-01	-6.00E-01	0.00E+00	4.37E+01	0.00E+00	-2.54E+01	0.00E+00
2.16E-01	-6.00E-01	0.00E+00	5.06E+01	0.00E+00	-2.97E+01	0.00E+00

**Table A-3
Trajectory Data, OH58D,
Test Point 14**

Time, Sec	x position, ft	y position, ft	z position, ft	psi, deg	theta, deg	phi, deg
0.1599999E-01	0.0000000E+00	0.0000000E+00	0.0000000E+00	0.0000000E+00	0.0000000E+00	0.0000000E+00
0.3999999E-01	0.0000000E+00	0.0000000E+00	0.2291667E+00	0.0000000E+00	-0.2250000E+01	0.0000000E+00
0.6399999E-01	0.0000000E+00	0.0000000E+00	0.6458333E+00	0.0000000E+00	-0.5000000E+01	0.0000000E+00
0.8799999E-01	-0.4166667E-01	0.0000000E+00	0.1083333E+01	0.0000000E+00	-0.7500000E+01	0.0000000E+00
0.1120000E+00	-0.4166667E-01	0.0000000E+00	0.1583333E+01	0.0000000E+00	-0.1225000E+02	0.0000000E+00
0.1370000E+00	-0.9166667E-01	0.0000000E+00	0.2070833E+01	0.0000000E+00	-0.1625000E+02	0.0000000E+00
0.1610000E+00	-0.9166667E-01	0.0000000E+00	0.2600000E+01	0.0000000E+00	-0.1900000E+02	0.0000000E+00
0.1850000E+00	-0.1208333E+00	0.0000000E+00	0.3141667E+01	0.0000000E+00	-0.2300000E+02	0.0000000E+00
0.2090000E+00	-0.1416667E+00	0.0000000E+00	0.3704167E+01	0.0000000E+00	-0.2675000E+02	0.0000000E+00
0.2330000E+00	-0.1708333E+00	0.0000000E+00	0.4254167E+01	0.7500000E+00	-0.3025000E+02	0.0000000E+00

**Table A-4
Trajectory Data, OH-58D,
Test Point15R**

Time, Sec	x position, ft	y position, ft	z position, ft	psi, deg	theta, deg	phi, deg
0.00E+00	0.00E+00	0.00E+00	0.00E+00	0.00E+00	0.00E+00	0.00E+00
2.40E-02	-6.00E-01	0.00E+00	2.60E+00	0.00E+00	0.00E+00	0.00E+00
4.80E-02	0.00E+00	0.00E+00	7.50E+00	0.00E+00	-4.00E+00	0.00E+00
7.20E-02	3.00E-01	0.00E+00	1.41E+01	0.00E+00	-7.00E+00	0.00E+00
9.60E-02	3.00E-01	0.00E+00	2.05E+01	0.00E+00	-1.15E+01	0.00E+00
1.20E-01	-4.00E-01	0.00E+00	2.64E+01	0.00E+00	-1.65E+01	0.00E+00
1.44E-01	-9.00E-01	0.00E+00	3.40E+01	0.00E+00	-2.00E+01	0.00E+00
1.68E-01	-1.50E+00	0.00E+00	4.02E+01	0.00E+00	-2.30E+01	0.00E+00
1.92E-01	-1.30E+00	0.00E+00	4.50E+01	0.00E+00	-2.60E+01	0.00E+00
2.16E-01	-3.00E-01	0.00E+00	4.89E+01	0.00E+00	-3.05E+01	0.00E+00

**Table A-5
Trajectory Data, OH-58D,
Test Point 16R**

Time, Sec	x position, ft	y position, ft	z position, ft	psi, deg	theta, deg	phi, deg
0.00E+00	0.00E+00	0.00E+00	0.00E+00	0.00E+00	0.00E+00	0.00E+00
2.40E-02	-8.00E-01	0.00E+00	7.00E-01	0.00E+00	-6.00E-01	0.00E+00
4.80E-02	-1.90E+00	0.00E+00	5.70E+00	0.00E+00	-3.90E+00	0.00E+00
7.20E-02	-1.40E+00	0.00E+00	1.13E+01	0.00E+00	-7.50E+00	0.00E+00
9.60E-02	-1.40E+00	0.00E+00	1.71E+01	0.00E+00	-1.25E+01	0.00E+00
1.20E-01	-1.20E+00	0.00E+00	2.33E+01	0.00E+00	-1.61E+01	0.00E+00
1.44E-01	-1.70E+00	0.00E+00	3.00E+01	0.00E+00	-2.00E+01	0.00E+00
1.68E-01	-3.10E+00	0.00E+00	3.74E+01	0.00E+00	-2.55E+01	0.00E+00
1.92E-01	-2.60E+00	0.00E+00	4.39E+01	0.00E+00	-2.90E+01	0.00E+00
2.16E-01	-3.30E+00	0.00E+00	5.13E+01	0.00E+00	-3.30E+01	0.00E+00

**Table A-6
Trajectory Data, OH-58D,
Test Point 17**

Time, Sec	x position, ft	y position, ft	z position, ft	psi, deg	theta, deg	phi, deg
0.200000E-01	0.000000E+00	0.000000E+00	0.000000E+00	0.000000E+00	0.000000E+00	0.000000E+00
0.440000E-01	-0.833333E-01	0.000000E+00	0.320833E+00	0.000000E+00	-0.325000E+01	0.000000E+00
0.660000E-01	-0.145833E+00	0.000000E+00	0.787500E+00	0.000000E+00	-0.715000E+01	0.000000E+00
0.660000E-01	-0.145833E+00	0.000000E+00	0.787500E+00	0.000000E+00	-0.715000E+01	0.000000E+00
0.116000E+00	-0.145833E+00	0.000000E+00	0.173333E+01	0.000000E+00	-0.161500E+02	0.000000E+00
0.140000E+00	-0.145833E+00	0.000000E+00	0.227916E+01	0.000000E+00	-0.196500E+02	0.000000E+00
0.164000E+00	-0.250000E+00	0.000000E+00	0.280833E+01	0.000000E+00	-0.232000E+02	0.000000E+00
0.188000E+00	-0.250000E+00	0.000000E+00	0.337083E+01	0.000000E+00	-0.282000E+02	0.000000E+00
0.212000E+00	-0.333333E+00	0.000000E+00	0.401250E+01	0.000000E+00	-0.329500E+02	0.000000E+00
0.236000E+00	-0.408333E+00	0.000000E+00	0.463333E+01	0.000000E+00	-0.372500E+02	0.000000E+00

**Table A-7
Trajectory Data, OH-58D,
Test Point 18**

Time, Sec	x position, ft	y position, ft	z position, ft	psi, deg	theta, deg	phi, deg
0.160000E-01	0.000000E+00	0.000000E+00	0.000000E+00	0.000000E+00	0.000000E+00	0.000000E+00
0.450000E-01	-0.583333E-01	0.000000E+00	0.354166E+00	0.000000E+00	-0.250000E+01	0.000000E+00
0.730000E-01	-0.583333E-01	0.000000E+00	0.895833E+00	0.000000E+00	-0.685000E+01	0.000000E+00
0.100000E+00	-0.791666E-01	0.000000E+00	0.142083E+01	0.000000E+00	-0.111000E+02	0.000000E+00
0.128000E+00	-0.791666E-01	0.000000E+00	0.201250E+01	0.000000E+00	-0.160000E+02	0.000000E+00
0.155000E+00	-0.108333E+00	0.000000E+00	0.265833E+01	0.000000E+00	-0.206000E+02	0.000000E+00
0.182000E+00	-0.108333E+00	0.000000E+00	0.328333E+01	0.000000E+00	-0.249500E+02	0.000000E+00
0.208000E+00	-0.170833E+00	0.000000E+00	0.395000E+01	0.000000E+00	-0.292000E+02	0.000000E+00
0.234000E+00	-0.233333E+00	0.000000E+00	0.461666E+01	0.250000E+00	-0.344500E+02	0.000000E+00
0.261000E+00	-0.283333E+00	0.000000E+00	0.527083E+01	0.250000E+00	-0.384500E+02	0.000000E+00

**Table A-8
Trajectory Data, OH-58D,
Test Point 21**

Time, Sec	x position, ft	y position, ft	z position, ft	psi, deg	theta, deg	phi, deg
0.210000E-01	0.000000E+00	0.000000E+00	0.000000E+00	0.000000E+00	0.000000E+00	0.000000E+00
0.450000E-01	0.000000E+00	0.000000E+00	0.333333E+00	0.000000E+00	-0.225000E+01	0.000000E+00
0.690000E-01	-0.166667E-01	0.000000E+00	0.833333E+00	0.000000E+00	-0.655000E+01	0.000000E+00
0.929999E-01	-0.958333E-01	0.000000E+00	0.123750E+01	0.000000E+00	-0.100500E+02	0.000000E+00
0.117000E+00	-0.875000E-01	0.000000E+00	0.175000E+01	0.000000E+00	-0.153000E+02	0.000000E+00
0.141000E+00	-0.170833E+00	0.000000E+00	0.227083E+01	0.000000E+00	-0.183000E+02	0.000000E+00
0.165000E+00	-0.170833E+00	0.000000E+00	0.287500E+01	0.000000E+00	-0.250500E+02	0.000000E+00
0.189000E+00	-0.229167E+00	0.000000E+00	0.350417E+01	0.250000E+00	-0.288000E+02	0.000000E+00
0.213000E+00	-0.291667E+00	0.000000E+00	0.415000E+01	0.250000E+00	-0.340500E+02	0.000000E+00
0.237000E+00	-0.362500E+00	0.000000E+00	0.472917E+01	0.250000E+00	-0.386500E+02	0.000000E+00

**Table A-9
Trajectory Data, OH-58D,
Test Point 22**

Time, Sec	x position, ft	y position, ft	z position, ft	psi, deg	theta, deg	phi, deg
0.250000E-01	0.000000E+00	0.000000E+00	0.000000E+00	0.000000E+00	0.000000E+00	0.000000E+00
0.490000E-01	-0.125000E+00	0.000000E+00	0.420833E+00	0.000000E+00	-0.350000E+01	0.000000E+00
0.730000E-01	-0.133333E+00	0.000000E+00	0.854167E+00	0.000000E+00	-0.750000E+01	0.000000E+00
0.970000E-01	-0.183333E+00	0.000000E+00	0.142083E+01	0.000000E+00	-0.122000E+02	0.000000E+00
0.121000E+00	-0.225000E+00	0.000000E+00	0.193750E+01	0.000000E+00	-0.169500E+02	0.000000E+00
0.145000E+00	-0.266667E+00	0.000000E+00	0.247917E+01	0.000000E+00	-0.217000E+02	0.000000E+00
0.169000E+00	-0.345833E+00	0.000000E+00	0.300000E+01	0.000000E+00	-0.265500E+02	0.000000E+00

**Table A-10
Trajectory Data, OH-58D,
Test Point 23**

Time, Sec	x position, ft	y position, ft	z position, ft	psi, deg	theta, deg	phi, deg
0.185000E-01	0.000000E+00	0.000000E+00	0.000000E+00	0.000000E+00	0.000000E+00	0.000000E+00
0.425000E-01	-0.541667E-01	0.000000E+00	0.287500E+00	0.000000E+00	-0.245000E+01	0.000000E+00
0.665000E-01	-0.875000E-01	0.000000E+00	0.758333E+00	0.000000E+00	-0.630000E+01	0.000000E+00
0.905000E-01	-0.875000E-01	0.000000E+00	0.123750E+01	0.000000E+00	-0.108000E+02	0.000000E+00
0.114500E+00	-0.129167E+00	0.000000E+00	0.174583E+01	0.000000E+00	-0.154000E+02	0.000000E+00
0.138500E+00	-0.200000E+00	0.000000E+00	0.228333E+01	0.000000E+00	-0.209000E+02	0.000000E+00
0.162500E+00	-0.237500E+00	0.000000E+00	0.284583E+01	0.000000E+00	-0.263500E+02	0.000000E+00
0.186500E+00	-0.341667E+00	0.000000E+00	0.340833E+01	0.000000E+00	-0.323500E+02	0.000000E+00
0.210500E+00	-0.404167E+00	0.000000E+00	0.403333E+01	0.000000E+00	-0.386000E+02	0.000000E+00

APPENDIX B
TRAJECTORIES FROM OH-13 SCALE MODEL JETTISON TEST

APPENDIX B

TRAJECTORIES FROM OH-13 SCALE MODEL JETTISON TEST

Table B-1. Scale Model Test, 40 Knots Full-Scale Velocity, Digital Camera

Fm#	Timestamp	X Position (in)	Y Position (in)	Z Position (in)	Psi (yaw) (deg)	Theta (pitch) (deg)	Phi (roll) (deg)
0	56.295	0.00E+00	0.00E+00	0.00E+00	0.00E+00	0.00E+00	0.00E+00
1	56.298	0.00E+00	0.00E+00	0.00E+00	0.00E+00	0.00E+00	0.00E+00
2	56.3	0.00E+00	0.00E+00	0.00E+00	0.00E+00	0.00E+00	0.00E+00
3	56.303	0.00E+00	0.00E+00	0.00E+00	0.00E+00	-5.00E-01	0.00E+00
4	56.305	0.00E+00	0.00E+00	5.00E-01	0.00E+00	-1.25E+00	0.00E+00
5	56.308	0.00E+00	0.00E+00	7.50E-01	0.00E+00	-1.75E+00	0.00E+00
6	56.31	0.00E+00	0.00E+00	1.00E+00	0.00E+00	-2.50E+00	0.00E+00
7	56.313	2.50E-01	-2.50E-01	1.30E+00	0.00E+00	-2.50E+00	0.00E+00
8	56.315	2.50E-01	-2.50E-01	1.65E+00	0.00E+00	-2.75E+00	0.00E+00
9	56.318	2.50E-01	-2.50E-01	1.90E+00	0.00E+00	-3.00E+00	0.00E+00
10	56.32	7.50E-01	-5.00E-01	2.65E+00	0.00E+00	-3.25E+00	0.00E+00
11	56.323	7.00E-01	-2.50E-01	2.65E+00	0.00E+00	-4.00E+00	0.00E+00
12	56.325	7.00E-01	-2.50E-01	2.95E+00	0.00E+00	-4.25E+00	0.00E+00
13	56.328	6.00E-01	-2.50E-01	2.95E+00	0.00E+00	-4.25E+00	0.00E+00
14	56.33	6.00E-01	-2.50E-01	3.15E+00	0.00E+00	-4.95E+00	0.00E+00
15	56.333	6.00E-01	-2.50E-01	3.35E+00	0.00E+00	-5.05E+00	0.00E+00
16	56.335	6.00E-01	-2.50E-01	3.75E+00	0.00E+00	-5.55E+00	0.00E+00
17	56.338	6.00E-01	-2.50E-01	3.85E+00	0.00E+00	-5.80E+00	0.00E+00
18	56.34	6.00E-01	-2.50E-01	4.05E+00	0.00E+00	-6.45E+00	0.00E+00
19	56.343	6.00E-01	-2.50E-01	4.25E+00	0.00E+00	-6.65E+00	0.00E+00
20	56.345	6.00E-01	-2.50E-01	4.65E+00	0.00E+00	-7.20E+00	0.00E+00
21	56.348	6.00E-01	-2.50E-01	4.95E+00	0.00E+00	-7.50E+00	0.00E+00
22	56.35	6.00E-01	-2.50E-01	5.25E+00	0.00E+00	-7.65E+00	0.00E+00
23	56.353	6.00E-01	-2.50E-01	5.55E+00	0.00E+00	-8.15E+00	0.00E+00
24	56.355	6.00E-01	-4.50E-01	5.95E+00	0.00E+00	-8.55E+00	0.00E+00
25	56.358	6.00E-01	-4.50E-01	6.15E+00	0.00E+00	-8.85E+00	0.00E+00
26	56.36	6.00E-01	-4.50E-01	6.25E+00	0.00E+00	-9.25E+00	0.00E+00
27	56.363	6.00E-01	-4.50E-01	6.65E+00	0.00E+00	-1.01E+01	0.00E+00
28	56.365	6.00E-01	-5.50E-01	7.15E+00	0.00E+00	-1.09E+01	0.00E+00
29	56.368	5.00E-01	-5.50E-01	7.25E+00	-5.00E-01	-1.11E+01	0.00E+00
30	56.37	5.00E-01	-5.50E-01	7.55E+00	-5.00E-01	-1.15E+01	0.00E+00
31	56.373	5.00E-01	-5.50E-01	7.95E+00	-5.00E-01	-1.22E+01	0.00E+00
32	56.375	5.00E-01	-5.50E-01	8.15E+00	-5.00E-01	-1.23E+01	0.00E+00
33	56.378	5.00E-01	-5.50E-01	8.45E+00	-5.00E-01	-1.27E+01	0.00E+00
34	56.38	5.00E-01	-5.50E-01	8.75E+00	-5.00E-01	-1.28E+01	0.00E+00
35	56.383	5.00E-01	-5.50E-01	9.05E+00	-5.00E-01	-1.31E+01	0.00E+00
36	56.385	7.00E-01	-5.50E-01	9.35E+00	-5.00E-01	-1.34E+01	0.00E+00
37	56.388	7.00E-01	-1.50E-01	9.25E+00	-1.49E-08	-1.35E+01	0.00E+00
38	56.39	7.00E-01	-1.50E-01	9.35E+00	-1.49E-08	-1.39E+01	0.00E+00
39	56.393	7.00E-01	-1.50E-01	9.75E+00	-1.49E-08	-1.39E+01	0.00E+00
40	56.395	7.00E-01	-1.50E-01	1.01E+01	-1.49E-08	-1.41E+01	0.00E+00
41	56.398	7.00E-01	-2.50E-01	1.06E+01	-1.49E-08	-1.45E+01	0.00E+00
42	56.4	7.00E-01	-2.50E-01	1.08E+01	-1.49E-08	-1.54E+01	0.00E+00
43	56.403	7.00E-01	5.00E-02	1.11E+01	-1.49E-08	-1.60E+01	0.00E+00
44	56.405	6.00E-01	5.00E-02	1.15E+01	-1.49E-08	-1.63E+01	0.00E+00
45	56.408	6.00E-01	-5.00E-02	1.19E+01	-1.49E-08	-1.72E+01	0.00E+00
46	56.41	6.00E-01	-5.00E-02	1.22E+01	-1.49E-08	-1.75E+01	0.00E+00
47	56.413	7.00E-01	5.00E-02	1.27E+01	-1.49E-08	-1.80E+01	0.00E+00
48	56.415	7.00E-01	5.00E-02	1.30E+01	-1.49E-08	-1.82E+01	0.00E+00
49	56.418	7.00E-01	5.00E-02	1.33E+01	-1.49E-08	-1.86E+01	0.00E+00
50	56.42	7.00E-01	5.00E-02	1.37E+01	-1.49E-08	-1.87E+01	0.00E+00
51	56.423	7.00E-01	5.00E-02	1.40E+01	-1.49E-08	-1.92E+01	0.00E+00
52	56.425	7.00E-01	5.00E-02	1.44E+01	-1.49E-08	-2.01E+01	0.00E+00
53	56.428	7.00E-01	5.00E-02	1.49E+01	-1.49E-08	-2.05E+01	0.00E+00
54	56.43	7.00E-01	5.00E-02	1.53E+01	-1.49E-08	-2.11E+01	0.00E+00
55	56.433	7.00E-01	2.50E-01	1.55E+01	-1.49E-08	-2.15E+01	0.00E+00
56	56.435	7.00E-01	2.50E-01	1.57E+01	-1.49E-08	-2.23E+01	0.00E+00
57	56.438	7.00E-01	2.50E-01	1.62E+01	-1.49E-08	-2.23E+01	0.00E+00
58	56.44	4.00E-01	2.50E-01	1.65E+01	-1.49E-08	-2.23E+01	0.00E+00
59	56.443	4.00E-01	2.50E-01	1.67E+01	-1.49E-08	-2.24E+01	0.00E+00
60	56.445	4.00E-01	2.50E-01	1.70E+01	-1.49E-08	-2.32E+01	-5.00E-01
61	56.448	4.00E-01	2.50E-01	1.75E+01	-1.49E-08	-2.36E+01	-5.00E-01

Table B-2. Scale Model Test, 70 Knots Full-Scale Velocity, Digital Camera

Fm#	Timestamp	X Position (in)	Y Position (in)	Z Position (in)	Psi (yaw) (deg)	Theta (pitch) (deg)	Phi (roll) (deg)
0	0	-1.49E-08	0.00E+00	0.00E+00	0.00E+00	0.00E+00	0.00E+00
1	0.0025	-1.49E-08	0.00E+00	0.00E+00	0.00E+00	0.00E+00	0.00E+00
2	0.005	-1.49E-08	0.00E+00	0.00E+00	0.00E+00	0.00E+00	0.00E+00
3	0.0075	-1.49E-08	0.00E+00	0.00E+00	0.00E+00	0.00E+00	0.00E+00
4	0.01	-1.49E-08	0.00E+00	0.00E+00	0.00E+00	0.00E+00	0.00E+00
5	0.0125	-1.49E-08	0.00E+00	0.00E+00	0.00E+00	0.00E+00	0.00E+00
6	0.015	-1.49E-08	0.00E+00	2.00E-01	0.00E+00	0.00E+00	0.00E+00
7	0.0175	-1.49E-08	0.00E+00	3.00E-01	0.00E+00	0.00E+00	0.00E+00
8	0.02	-1.49E-08	-2.00E-01	7.00E-01	0.00E+00	-1.20E+00	0.00E+00
9	0.0225	-1.49E-08	-2.00E-01	8.00E-01	0.00E+00	-1.20E+00	0.00E+00
10	0.025	2.00E-01	-4.00E-01	1.20E+00	0.00E+00	-1.20E+00	0.00E+00
11	0.0275	2.00E-01	-4.00E-01	1.20E+00	0.00E+00	-1.20E+00	0.00E+00
12	0.03	2.00E-01	-4.00E-01	1.20E+00	0.00E+00	-1.20E+00	0.00E+00
13	0.0325	2.00E-01	-4.00E-01	1.60E+00	0.00E+00	-1.60E+00	0.00E+00
14	0.035	4.00E-01	-8.00E-01	2.20E+00	-8.00E-01	-2.60E+00	0.00E+00
15	0.0375	4.00E-01	-8.00E-01	2.40E+00	-8.00E-01	-2.80E+00	0.00E+00
16	0.04	4.00E-01	-8.00E-01	2.60E+00	-8.00E-01	-3.40E+00	0.00E+00
17	0.0425	4.00E-01	-8.00E-01	3.00E+00	-8.00E-01	-3.80E+00	0.00E+00
18	0.045	6.00E-01	-1.00E+00	3.40E+00	-8.00E-01	-4.40E+00	0.00E+00
19	0.0475	8.00E-01	-1.20E+00	3.80E+00	-8.00E-01	-4.80E+00	0.00E+00
20	0.05	8.00E-01	-1.40E+00	4.20E+00	-8.00E-01	-5.80E+00	0.00E+00
21	0.0525	1.00E+00	-1.40E+00	4.60E+00	-8.00E-01	-5.80E+00	0.00E+00
22	0.055	1.00E+00	-1.40E+00	4.80E+00	-8.00E-01	-5.80E+00	0.00E+00
23	0.0575	1.00E+00	-1.60E+00	5.00E+00	-8.00E-01	-6.00E+00	0.00E+00
24	0.06	1.20E+00	-1.60E+00	5.40E+00	-6.00E-01	-5.80E+00	0.00E+00
25	0.0625	1.20E+00	-1.60E+00	5.80E+00	-6.00E-01	-6.40E+00	0.00E+00
26	0.065	1.40E+00	-1.80E+00	6.40E+00	-2.00E-01	-7.20E+00	0.00E+00
27	0.0675	1.40E+00	-1.80E+00	6.80E+00	-2.00E-01	-7.60E+00	0.00E+00
28	0.07	1.70E+00	-2.20E+00	7.40E+00	-2.00E-01	-7.80E+00	0.00E+00
29	0.0725	1.90E+00	-2.20E+00	7.60E+00	-2.00E-01	-8.00E+00	0.00E+00
30	0.075	1.90E+00	-2.20E+00	7.80E+00	7.45E-08	-8.00E+00	0.00E+00
31	0.0775	1.90E+00	-2.20E+00	8.00E+00	7.45E-08	-8.00E+00	0.00E+00
32	0.08	1.90E+00	-2.20E+00	8.20E+00	7.45E-08	-8.40E+00	0.00E+00
33	0.0825	1.90E+00	-2.20E+00	8.40E+00	7.45E-08	-8.40E+00	0.00E+00
34	0.085	2.10E+00	-2.40E+00	8.80E+00	5.00E-01	-8.40E+00	0.00E+00
35	0.0875	2.30E+00	-2.40E+00	9.20E+00	5.00E-01	-8.60E+00	0.00E+00
36	0.09	2.30E+00	-2.40E+00	9.40E+00	5.00E-01	-8.60E+00	0.00E+00
37	0.0925	2.30E+00	-2.40E+00	9.70E+00	5.00E-01	-9.00E+00	0.00E+00
38	0.095	2.30E+00	-2.40E+00	1.01E+01	5.00E-01	-9.50E+00	0.00E+00
39	0.0975	2.50E+00	-2.60E+00	1.04E+01	7.00E-01	-9.50E+00	0.00E+00
40	0.1	2.50E+00	-2.60E+00	1.08E+01	7.00E-01	-1.03E+01	0.00E+00
41	0.1025	2.50E+00	-2.60E+00	1.12E+01	7.00E-01	-1.11E+01	0.00E+00
42	0.105	2.40E+00	-2.60E+00	1.16E+01	7.00E-01	-1.17E+01	0.00E+00
43	0.1075	2.40E+00	-2.60E+00	1.16E+01	7.00E-01	-1.19E+01	0.00E+00
44	0.11	2.40E+00	-2.60E+00	1.20E+01	7.00E-01	-1.23E+01	0.00E+00
45	0.1125	2.20E+00	-2.60E+00	1.20E+01	1.10E+00	-1.32E+01	0.00E+00
46	0.115	2.20E+00	-2.60E+00	1.24E+01	1.10E+00	-1.32E+01	0.00E+00
47	0.1175	2.40E+00	-2.60E+00	1.28E+01	1.10E+00	-1.38E+01	0.00E+00
48	0.12	2.60E+00	-2.60E+00	1.32E+01	9.00E-01	-1.38E+01	0.00E+00
49	0.1225	2.50E+00	-2.60E+00	1.36E+01	1.50E+00	-1.42E+01	0.00E+00
50	0.125	2.50E+00	-2.60E+00	1.39E+01	1.50E+00	-1.49E+01	0.00E+00
51	0.1275	2.50E+00	-2.60E+00	1.41E+01	1.50E+00	-1.49E+01	0.00E+00
52	0.13	2.50E+00	-2.60E+00	1.45E+01	1.50E+00	-1.57E+01	0.00E+00
53	0.1325	2.50E+00	-2.60E+00	1.47E+01	2.10E+00	-1.59E+01	0.00E+00
54	0.135	2.50E+00	-2.60E+00	1.51E+01	2.10E+00	-1.63E+01	0.00E+00
55	0.1375	2.70E+00	-2.60E+00	1.53E+01	2.10E+00	-1.63E+01	0.00E+00
56	0.14	2.70E+00	-2.60E+00	1.59E+01	2.10E+00	-1.69E+01	0.00E+00
57	0.1425	2.60E+00	-2.60E+00	1.63E+01	2.10E+00	-1.77E+01	0.00E+00
58	0.145	2.60E+00	-2.60E+00	1.65E+01	2.10E+00	-1.77E+01	0.00E+00
59	0.1475	2.80E+00	-2.60E+00	1.71E+01	2.10E+00	-1.85E+01	0.00E+00
60	0.15	2.80E+00	-2.60E+00	1.75E+01	2.10E+00	-1.89E+01	0.00E+00
61	0.1525	2.80E+00	-2.60E+00	1.79E+01	2.10E+00	-1.89E+01	0.00E+00

Table B-3. Scale Model Test, 70 Knots Full-Scale Velocity, Film Camera

Fm#	Timestamp	X Position (in)	Y Position (in)	Z Position (in)	Psi (yaw) (deg)	Theta (pitch) (deg)	Phi (roll) (deg)
0	0	0.00E+00	0.00E+00	0.00E+00	0.00E+00	0.00E+00	0.00E+00
1	0.0025	0.00E+00	0.00E+00	0.00E+00	0.00E+00	0.00E+00	0.00E+00
2	0.005	0.00E+00	0.00E+00	0.00E+00	0.00E+00	0.00E+00	0.00E+00
3	0.0075	0.00E+00	0.00E+00	0.00E+00	0.00E+00	0.00E+00	0.00E+00
4	0.01	0.00E+00	0.00E+00	0.00E+00	0.00E+00	0.00E+00	0.00E+00
5	0.0125	0.00E+00	0.00E+00	0.00E+00	0.00E+00	0.00E+00	0.00E+00
6	0.015	0.00E+00	0.00E+00	5.00E-01	0.00E+00	0.00E+00	0.00E+00
7	0.0175	0.00E+00	0.00E+00	5.00E-01	0.00E+00	0.00E+00	0.00E+00
8	0.02	0.00E+00	0.00E+00	9.00E-01	0.00E+00	0.00E+00	0.00E+00
9	0.0225	0.00E+00	0.00E+00	1.00E+00	0.00E+00	0.00E+00	0.00E+00
10	0.025	0.00E+00	0.00E+00	1.60E+00	0.00E+00	-1.10E+00	0.00E+00
11	0.0275	0.00E+00	0.00E+00	1.80E+00	0.00E+00	-1.10E+00	0.00E+00
12	0.03	0.00E+00	0.00E+00	1.90E+00	0.00E+00	-1.10E+00	0.00E+00
13	0.0325	0.00E+00	0.00E+00	2.30E+00	0.00E+00	-1.60E+00	0.00E+00
14	0.035	0.00E+00	0.00E+00	2.50E+00	0.00E+00	-2.00E+00	0.00E+00
15	0.0375	0.00E+00	0.00E+00	2.60E+00	0.00E+00	-2.30E+00	0.00E+00
16	0.04	0.00E+00	0.00E+00	2.80E+00	0.00E+00	-2.50E+00	0.00E+00
17	0.0425	3.00E-01	0.00E+00	2.90E+00	0.00E+00	-2.60E+00	0.00E+00
18	0.045	3.00E-01	0.00E+00	3.10E+00	0.00E+00	-3.30E+00	0.00E+00
19	0.0475	3.00E-01	0.00E+00	3.20E+00	3.00E-01	-3.70E+00	0.00E+00
20	0.05	3.00E-01	0.00E+00	3.40E+00	3.00E-01	-3.90E+00	0.00E+00
21	0.0525	3.00E-01	0.00E+00	3.50E+00	3.00E-01	-4.50E+00	0.00E+00
22	0.055	3.00E-01	0.00E+00	3.80E+00	3.00E-01	-4.80E+00	0.00E+00
23	0.0575	1.00E-01	0.00E+00	4.00E+00	3.00E-01	-5.70E+00	0.00E+00
24	0.06	1.00E-01	0.00E+00	4.00E+00	3.00E-01	-6.00E+00	0.00E+00
25	0.0625	1.49E-08	0.00E+00	4.00E+00	3.00E-01	-6.80E+00	0.00E+00
26	0.065	1.49E-08	0.00E+00	4.30E+00	3.00E-01	-7.20E+00	0.00E+00
27	0.0675	-1.00E-01	0.00E+00	4.50E+00	3.00E-01	-7.50E+00	0.00E+00
28	0.07	-1.00E-01	0.00E+00	4.60E+00	3.00E-01	-7.80E+00	0.00E+00
29	0.0725	-1.00E-01	0.00E+00	4.40E+00	3.00E-01	-7.20E+00	0.00E+00
30	0.075	-1.00E-01	0.00E+00	4.60E+00	3.00E-01	-7.20E+00	0.00E+00
31	0.0775	-1.00E-01	0.00E+00	5.00E+00	3.00E-01	-7.60E+00	0.00E+00
32	0.08	2.00E-01	-1.00E-01	5.60E+00	3.00E-01	-9.30E+00	0.00E+00
33	0.0825	2.00E-01	0.00E+00	5.60E+00	3.00E-01	-9.30E+00	0.00E+00
34	0.085	-1.00E-01	0.00E+00	5.80E+00	3.00E-01	-9.30E+00	0.00E+00
35	0.0875	2.00E-01	-1.00E-01	6.20E+00	3.00E-01	-9.80E+00	0.00E+00
36	0.09	2.00E-01	-1.00E-01	6.70E+00	3.00E-01	-1.04E+01	0.00E+00
37	0.0925	4.00E-01	-1.00E-01	7.50E+00	3.00E-01	-1.10E+01	0.00E+00
38	0.095	4.00E-01	-4.00E-01	7.50E+00	3.00E-01	-1.10E+01	0.00E+00
39	0.0975	5.00E-01	-4.00E-01	7.80E+00	3.00E-01	-1.14E+01	0.00E+00
40	0.1	5.00E-01	-4.00E-01	8.10E+00	3.00E-01	-1.18E+01	0.00E+00
41	0.1025	5.00E-01	-4.00E-01	8.40E+00	3.00E-01	-1.19E+01	0.00E+00
42	0.105	5.00E-01	-4.00E-01	8.80E+00	3.00E-01	-1.22E+01	0.00E+00
43	0.1075	5.00E-01	-4.00E-01	9.00E+00	3.00E-01	-1.24E+01	0.00E+00
44	0.11	6.00E-01	-4.00E-01	9.90E+00	3.00E-01	-1.34E+01	0.00E+00
45	0.1125	6.00E-01	-4.00E-01	9.90E+00	-5.00E-01	-1.28E+01	0.00E+00
46	0.115	6.00E-01	-4.00E-01	1.00E+01	-5.00E-01	-1.28E+01	0.00E+00
47	0.1175	8.00E-01	-8.00E-01	1.03E+01	-5.00E-01	-1.28E+01	0.00E+00
48	0.12	8.00E-01	-8.00E-01	1.05E+01	-5.00E-01	-1.30E+01	0.00E+00
49	0.1225	8.00E-01	-8.00E-01	1.06E+01	-5.00E-01	-1.30E+01	0.00E+00
50	0.125	8.00E-01	-8.00E-01	1.10E+01	-5.00E-01	-1.30E+01	0.00E+00
51	0.1275	9.00E-01	-8.00E-01	1.10E+01	-5.00E-01	-1.32E+01	0.00E+00
52	0.13	9.00E-01	-8.00E-01	1.11E+01	-5.00E-01	-1.32E+01	0.00E+00
53	0.1325	9.00E-01	-8.00E-01	1.11E+01	-5.00E-01	-1.35E+01	0.00E+00
54	0.135	9.00E-01	-8.00E-01	1.13E+01	-5.00E-01	-1.41E+01	0.00E+00
55	0.1375	7.00E-01	-8.00E-01	1.16E+01	-5.00E-01	-1.43E+01	0.00E+00
56	0.14	7.00E-01	-8.00E-01	1.18E+01	-5.00E-01	-1.47E+01	0.00E+00
57	0.1425	8.00E-01	-8.00E-01	1.20E+01	-5.00E-01	-1.51E+01	0.00E+00
58	0.145	8.00E-01	-8.00E-01	1.21E+01	-5.00E-01	-1.54E+01	0.00E+00
59	0.1475	5.00E-01	-8.00E-01	1.22E+01	-5.00E-01	-1.58E+01	0.00E+00
60	0.15	5.00E-01	-8.00E-01	1.23E+01	-5.00E-01	-1.59E+01	0.00E+00
61	0.1525	5.00E-01	-8.00E-01	1.25E+01	-5.00E-01	-1.62E+01	0.00E+00
62	0.155	5.00E-01	-8.00E-01	1.26E+01	-5.00E-01	-1.63E+01	0.00E+00
63	0.1575	5.00E-01	-8.00E-01	1.31E+01	-5.00E-01	-1.67E+01	0.00E+00
64	0.16	5.00E-01	-8.00E-01	1.34E+01	-5.00E-01	-1.68E+01	0.00E+00
65	0.1625	3.00E-01	-8.00E-01	1.35E+01	-5.00E-01	-1.71E+01	0.00E+00
66	0.165	3.00E-01	-8.00E-01	1.36E+01	-5.00E-01	-1.71E+01	0.00E+00
67	0.1675	3.00E-01	-8.00E-01	1.42E+01	-5.00E-01	-1.73E+01	0.00E+00
68	0.17	3.00E-01	-8.00E-01	1.46E+01	-5.00E-01	-1.75E+01	0.00E+00
69	0.1725	3.00E-01	-8.00E-01	1.51E+01	-5.00E-01	-1.79E+01	0.00E+00
70	0.175	3.00E-01	-8.00E-01	1.56E+01	-5.00E-01	-1.83E+01	0.00E+00
71	0.1775	3.00E-01	-8.00E-01	1.63E+01	-5.00E-01	-1.87E+01	0.00E+00
72	0.18	3.00E-01	-8.00E-01	1.67E+01	-5.00E-01	-1.87E+01	0.00E+00
73	0.1825	3.00E-01	-8.00E-01	1.70E+01	-5.00E-01	-1.91E+01	0.00E+00
74	0.185	3.00E-01	-8.00E-01	1.76E+01	-5.00E-01	-1.91E+01	0.00E+00
75	0.1875	3.00E-01	-8.00E-01	1.82E+01	-5.00E-01	-1.99E+01	0.00E+00
76	0.19	3.00E-01	-8.00E-01	1.88E+01	-5.00E-01	-1.99E+01	0.00E+00
77	0.1925	3.00E-01	-8.00E-01	1.90E+01	-5.00E-01	-2.02E+01	0.00E+00
78	0.195	3.00E-01	-8.00E-01	1.92E+01	-5.00E-01	-2.04E+01	0.00E+00

Table B-4. Scale Model Test, 100 Knots Full-Scale Velocity, Digital Camera

Fm#	Timestamp	X Position (in)	Y Position (in)	Z Position (in)	Psi (yaw) (deg)	Theta (pitch) (deg)	Phi (roll) (deg)
0	0	-1.60E+00	1.80E+00	-1.95E+00	3.00E-01	5.00E-02	0.00E+00
1	0.0025	-1.60E+00	1.80E+00	-1.95E+00	3.00E-01	5.00E-02	0.00E+00
2	0.005	-1.60E+00	1.80E+00	-1.95E+00	3.00E-01	5.00E-02	0.00E+00
3	0.0075	-1.60E+00	1.80E+00	-1.95E+00	3.00E-01	5.00E-02	0.00E+00
4	0.01	-1.60E+00	1.80E+00	-1.95E+00	3.00E-01	5.00E-02	0.00E+00
5	0.0125	-1.60E+00	1.80E+00	-1.95E+00	3.00E-01	5.00E-02	0.00E+00
6	0.015	-1.60E+00	1.80E+00	-1.75E+00	3.00E-01	-7.50E-01	0.00E+00
7	0.0175	-1.60E+00	1.80E+00	-1.65E+00	3.00E-01	-7.00E-01	0.00E+00
8	0.02	-1.60E+00	1.80E+00	-1.50E+00	3.00E-01	-1.45E+00	0.00E+00
9	0.0225	-1.60E+00	1.80E+00	-1.30E+00	3.00E-01	-1.40E+00	0.00E+00
10	0.025	-1.60E+00	1.80E+00	-1.00E+00	3.00E-01	-2.00E+00	0.00E+00
11	0.0275	-1.50E+00	1.60E+00	-6.00E-01	3.00E-01	-2.20E+00	0.00E+00
12	0.03	-1.60E+00	1.80E+00	-7.00E-01	3.00E-01	-2.20E+00	0.00E+00
13	0.0325	-1.40E+00	1.80E+00	-2.00E-01	3.00E-01	-3.10E+00	0.00E+00
14	0.035	-1.40E+00	1.80E+00	5.00E-02	3.00E-01	-3.20E+00	0.00E+00
15	0.0375	-1.40E+00	1.80E+00	3.00E-01	3.00E-01	-3.20E+00	0.00E+00
16	0.04	-1.40E+00	1.80E+00	6.00E-01	3.00E-01	-3.50E+00	0.00E+00
17	0.0425	-1.40E+00	1.80E+00	9.00E-01	3.00E-01	-4.00E+00	0.00E+00
18	0.045	-1.20E+00	1.80E+00	1.45E+00	3.00E-01	-5.10E+00	0.00E+00
19	0.0475	-1.20E+00	1.80E+00	1.75E+00	3.00E-01	-5.60E+00	0.00E+00
20	0.05	-1.30E+00	1.80E+00	1.85E+00	3.00E-01	-6.20E+00	0.00E+00
21	0.0525	-1.20E+00	1.80E+00	2.15E+00	3.00E-01	-6.60E+00	0.00E+00
22	0.055	-1.30E+00	1.80E+00	2.35E+00	3.00E-01	-7.00E+00	0.00E+00
23	0.0575	-1.30E+00	1.80E+00	2.75E+00	3.00E-01	-7.50E+00	0.00E+00
24	0.06	-1.50E+00	1.80E+00	2.75E+00	3.00E-01	-8.00E+00	0.00E+00
25	0.0625	-1.50E+00	1.70E+00	3.25E+00	3.00E-01	-8.50E+00	0.00E+00
26	0.065	-1.30E+00	1.50E+00	3.45E+00	3.00E-01	-8.50E+00	0.00E+00
27	0.0675	-1.30E+00	1.30E+00	3.85E+00	3.00E-01	-9.20E+00	0.00E+00
28	0.07	-9.00E-01	1.00E+00	4.65E+00	3.00E-01	-9.40E+00	0.00E+00
29	0.0725	-8.00E-01	8.00E-01	4.95E+00	3.00E-01	-1.04E+01	0.00E+00
30	0.075	-8.00E-01	8.00E-01	5.35E+00	5.00E-02	-1.11E+01	-5.05E+00
31	0.0775	-7.00E-01	8.00E-01	5.75E+00	5.00E-02	-1.16E+01	-5.05E+00
32	0.08	-7.00E-01	8.00E-01	6.05E+00	5.00E-02	-1.23E+01	-5.05E+00
33	0.0825	-5.00E-01	8.00E-01	6.35E+00	5.00E-02	-1.24E+01	-5.05E+00
34	0.085	-5.00E-01	8.00E-01	6.65E+00	5.00E-02	-1.30E+01	-5.05E+00
35	0.0875	-5.00E-01	8.00E-01	6.85E+00	5.00E-02	-1.35E+01	-5.05E+00
36	0.09	-5.00E-01	8.00E-01	7.15E+00	5.00E-02	-1.41E+01	-5.05E+00
37	0.0925	-7.00E-01	8.00E-01	7.55E+00	5.00E-02	-1.49E+01	-5.05E+00
38	0.095	-7.00E-01	8.00E-01	7.85E+00	5.00E-02	-1.52E+01	-5.05E+00
39	0.0975	-1.00E+00	8.00E-01	8.25E+00	5.00E-02	-1.66E+01	-5.05E+00
40	0.1	-8.00E-01	8.00E-01	8.45E+00	5.00E-02	-1.70E+01	-5.05E+00
41	0.1025	-4.00E-01	5.00E-01	9.15E+00	1.25E+00	-1.76E+01	-5.45E+00
42	0.105	-5.00E-01	5.00E-01	9.55E+00	1.30E+00	-1.79E+01	-5.45E+00
43	0.1075	-5.00E-01	5.00E-01	9.75E+00	1.30E+00	-1.80E+01	-5.45E+00
44	0.11	-5.00E-01	3.00E-01	1.02E+01	1.30E+00	-1.90E+01	-5.45E+00
45	0.1125	-5.00E-01	3.00E-01	1.06E+01	1.30E+00	-1.91E+01	-5.45E+00
46	0.115	-5.00E-01	3.00E-01	1.11E+01	1.50E+00	-2.05E+01	-5.45E+00
47	0.1175	-7.00E-01	3.00E-01	1.14E+01	1.50E+00	-2.11E+01	-5.45E+00
48	0.12	-6.00E-01	3.00E-01	1.17E+01	1.50E+00	-2.13E+01	-5.45E+00
49	0.1225	-6.00E-01	3.00E-01	1.21E+01	1.50E+00	-2.18E+01	-5.45E+00
50	0.125	-6.00E-01	3.00E-01	1.26E+01	1.50E+00	-2.28E+01	-5.45E+00
51	0.1275	-6.00E-01	3.00E-01	1.30E+01	1.50E+00	-2.36E+01	-5.45E+00
52	0.13	-7.00E-01	3.00E-01	1.33E+01	1.50E+00	-2.42E+01	-5.45E+00
53	0.1325	-7.00E-01	3.00E-01	1.37E+01	1.50E+00	-2.51E+01	-5.45E+00
54	0.135	-7.00E-01	3.00E-01	1.42E+01	1.50E+00	-2.60E+01	-5.45E+00

APPENDIX C
VERTICAL MOTION AND PITCH MOTION COMPARISON FIGURES

APPENDIX C
VERTICAL MOTION AND PITCH MOTION COMPARISON FIGURES

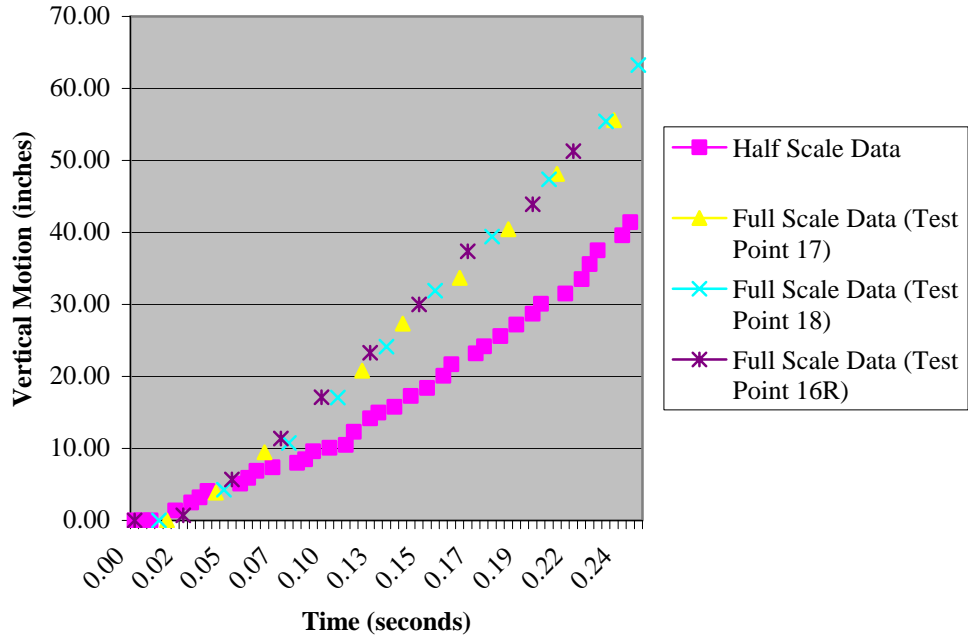


Figure C-1. Comparison of Vertical Motion at 70 Knots Full-Scale Conditions

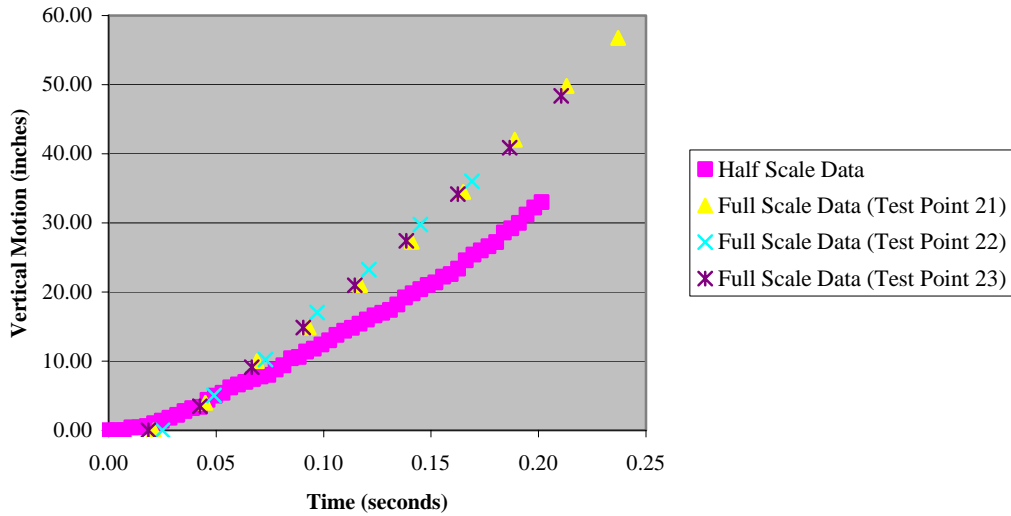


Figure C-2. Comparison of Vertical Motion at 100 Knots Full-Scale Conditions

APPENDIX D
COMPARISON OF PITCH MOTION CONDITIONS

APPENDIX D COMPARISON OF PITCH MOTION CONDITIONS

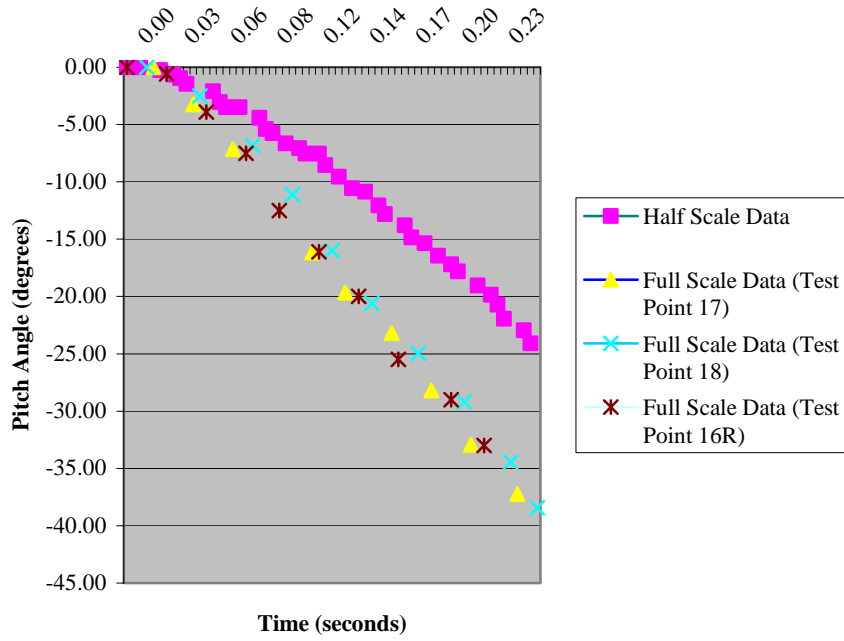


Figure D-1. Comparison of Pitch Motion at 70 Knots Full-Scale Conditions

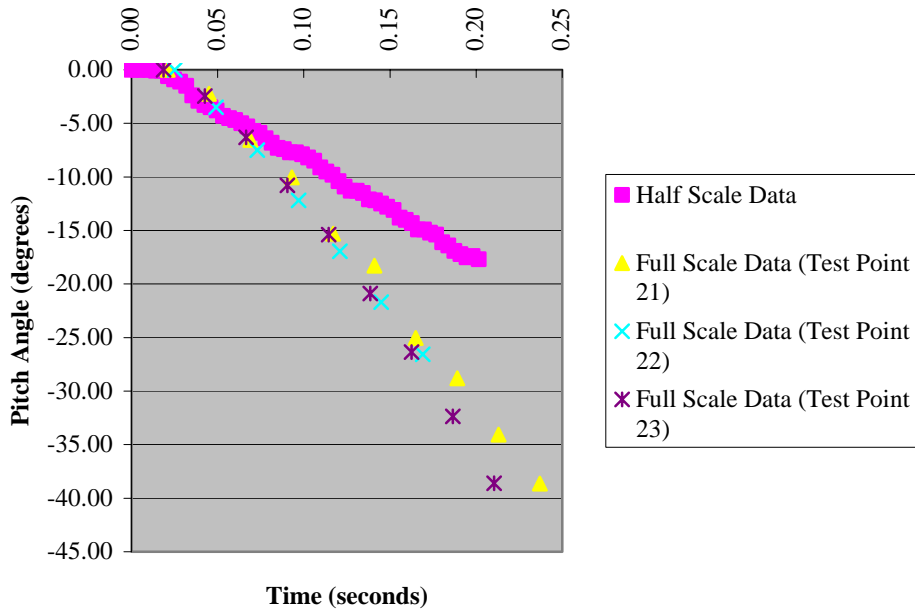


Figure D-2. Comparison of Pitch Motion at 100 Knots Full-Scale Conditions

APPENDIX E
COMPARISON OF MISS-DISTANCE

**APPENDIX E
COMPARISON OF MISS-DISTANCE**

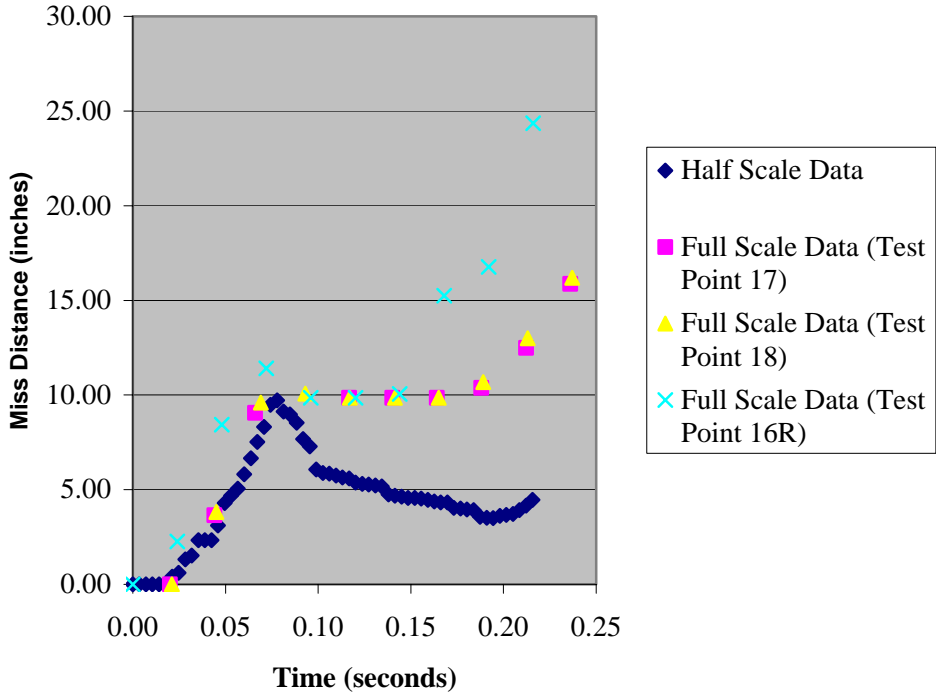


Figure E-1. Comparison of Miss-Distance Versus Time Calculation at 70 Knots Full-Scale Conditions

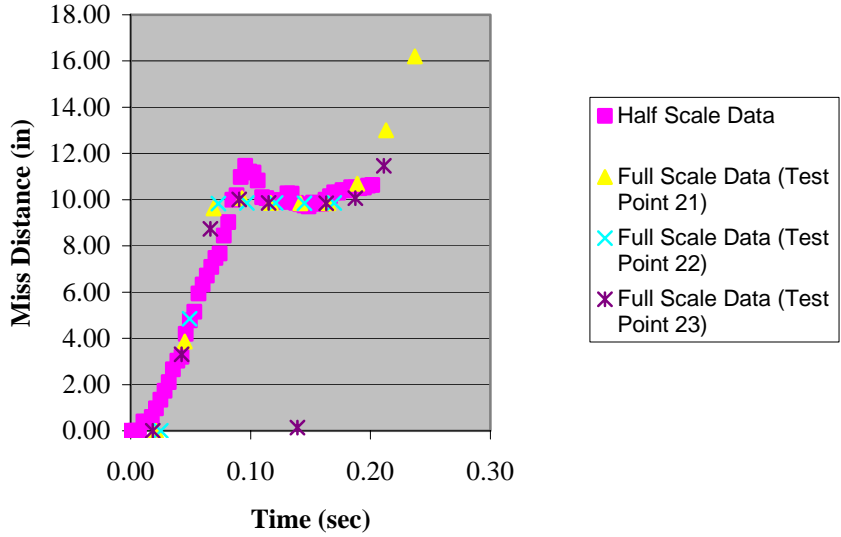


Figure E-2 Comparison of Miss-Distance Versus Time Calculation at 100 Knots Full-Scale Conditions

APPENDIX F
DOWNWASH ON VERTICAL MOTION AND PITCH MOTION FIGURES

APPENDIX F
DOWNWASH ON VERTICAL MOTION AND PITCH MOTION FIGURES

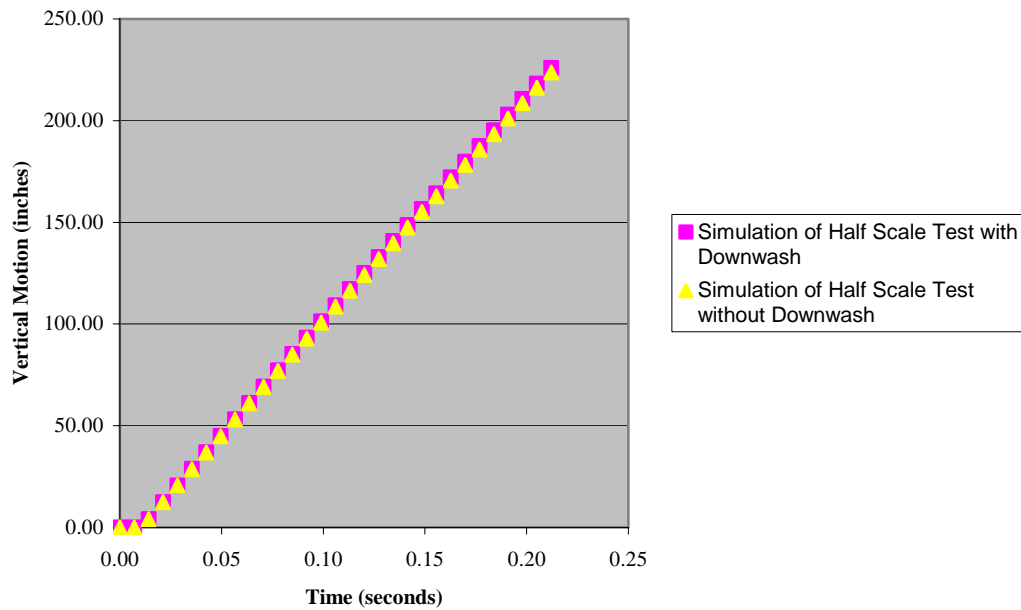


Figure F-1. Effect of Downwash on Vertical Motion, 40 Knots Full-Scale Conditions

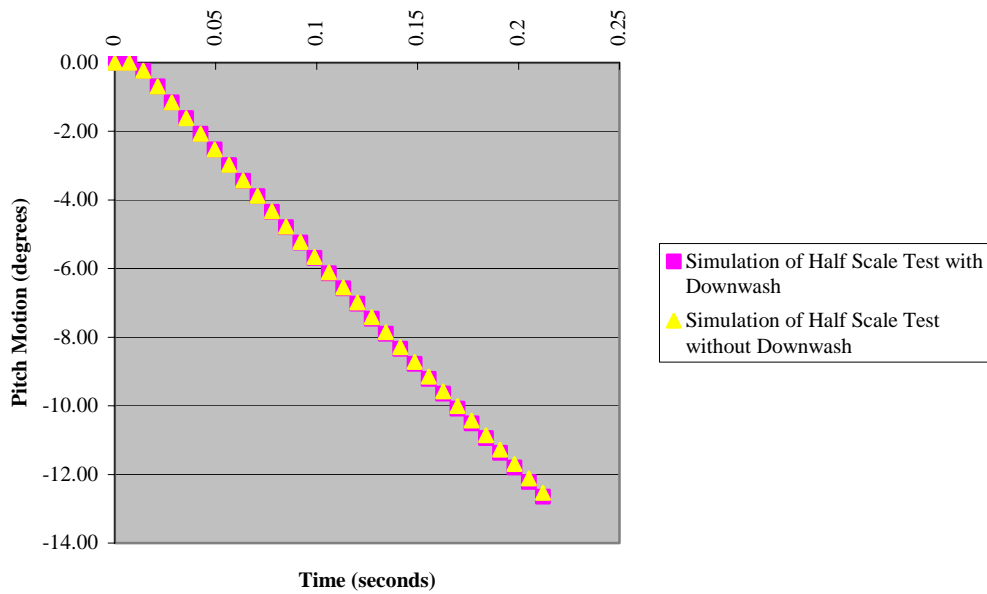


Figure F-2. Effect of Downwash on Pitch Motion, 40 Knots Full-Scale Conditions

APPENDIX G
BASELINE SIMULATION RESULTS

APPENDIX G BASELINE SIMULATION RESULTS

The charts in Appendix G are the baseline simulation results for the 70 knots full-scale condition and the 100 knots full-scale condition. The inputs are for the half-scale test as conducted, but without a rotor downwash input. The aircraft trim conditions are estimated from CASSAS ground camera data reduction results.

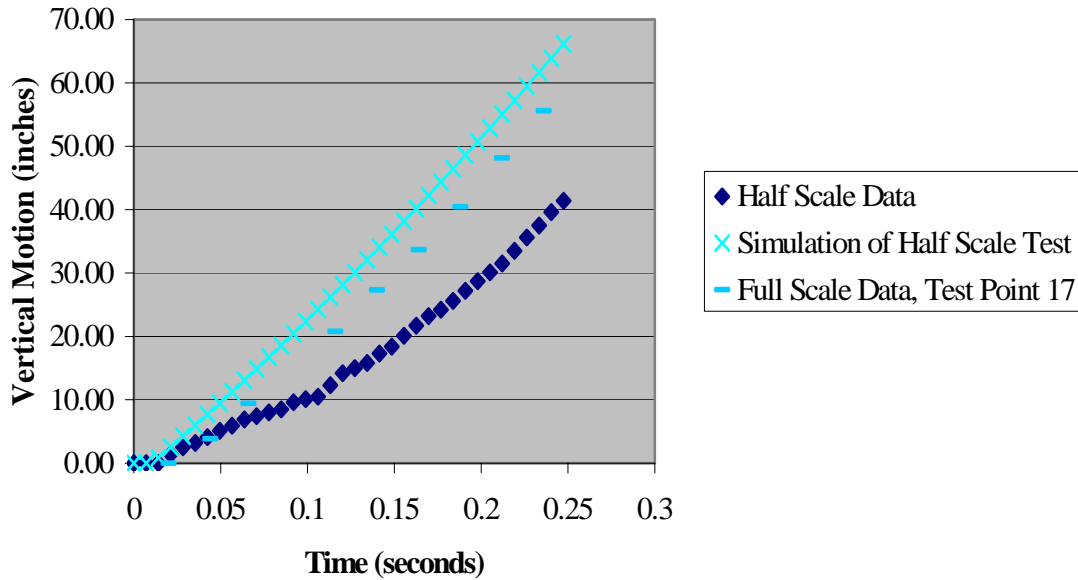


Figure G-1. Baseline Simulation Results, Vertical Motion, 70 Knots Full Scale-Conditions

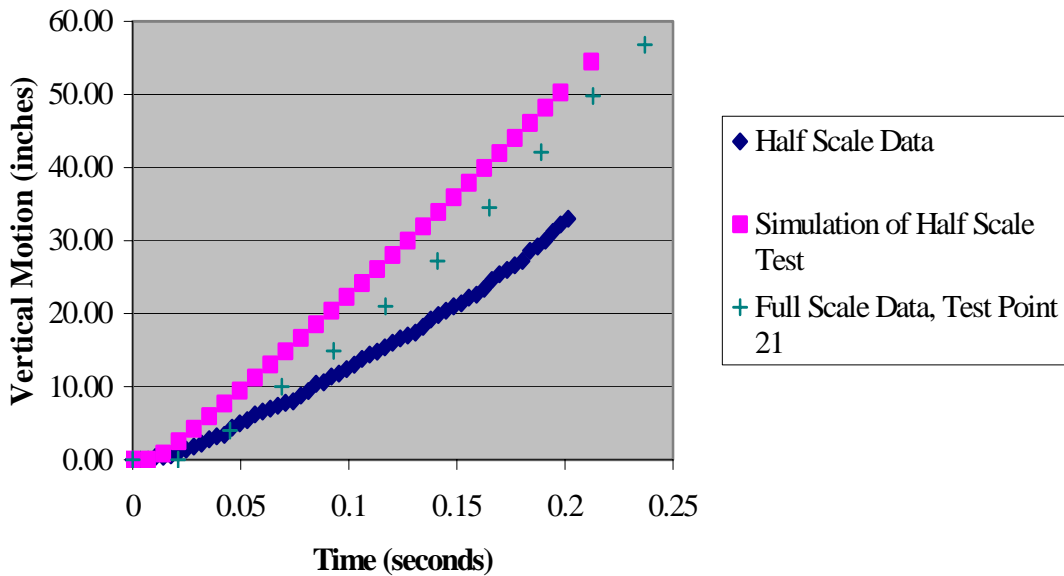


Figure G-2. Baseline Simulation Results, Vertical Motion, 100 Knots Full-Scale Conditions

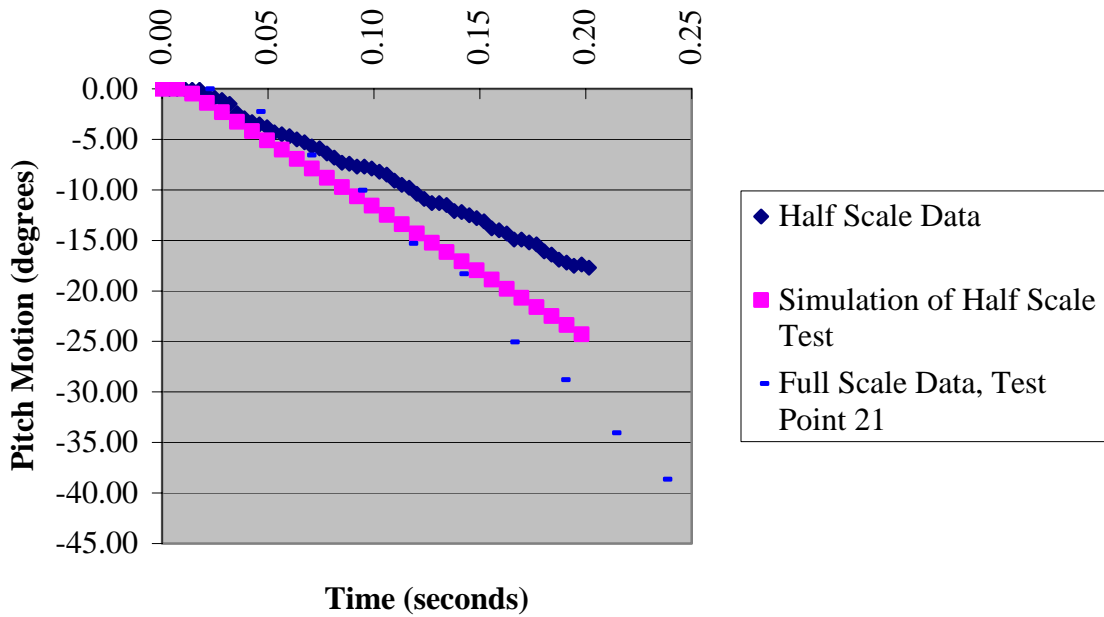


Figure G-3. Baseline Simulation Results, Pitch Motion, 70 Knots Full-Scale Conditions

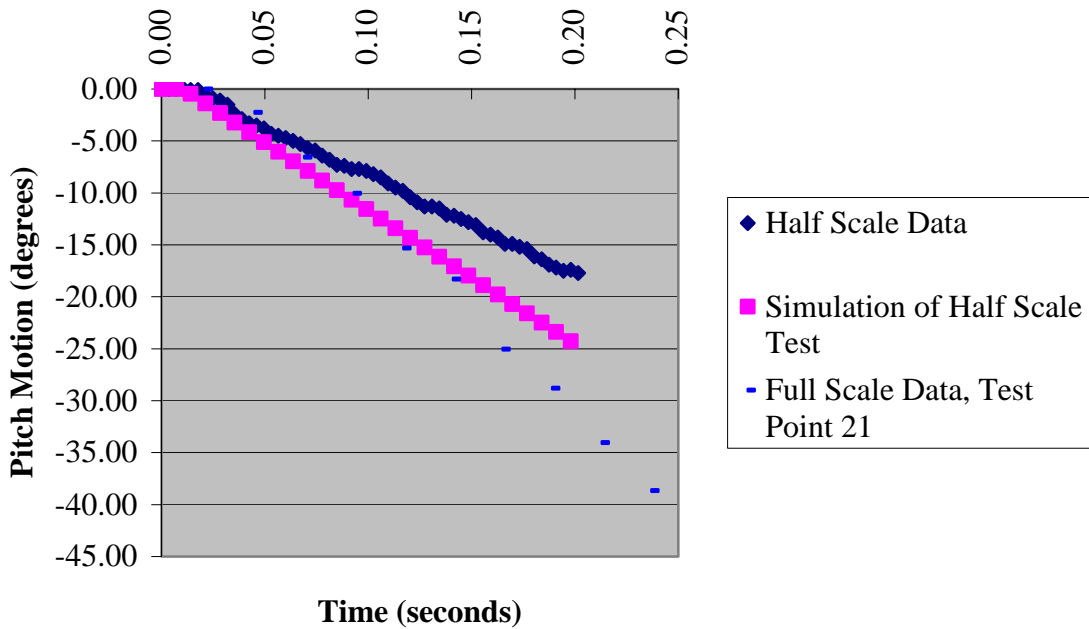


Figure G-4. Baseline Simulation Results, Pitch Motion, 100 Knots Full-Scale Conditions

APPENDIX H
EFFECT OF MOMENT OF INERTIA PLUS EJECTOR FORCE
CORRECTION ON PITCH MOTION AND VERTICAL MOTION

APPENDIX H
EFFECT OF MOMENT OF INERTIA PLUS EJECTOR FORCE
CORRECTION ON PITCH MOTION AND VERTICAL MOTION

Appendix H shows the results of simulating the half scale test with the moments of inertia and the ejector forces correctly scaled. These effects are generally cumulative for pitch motion.

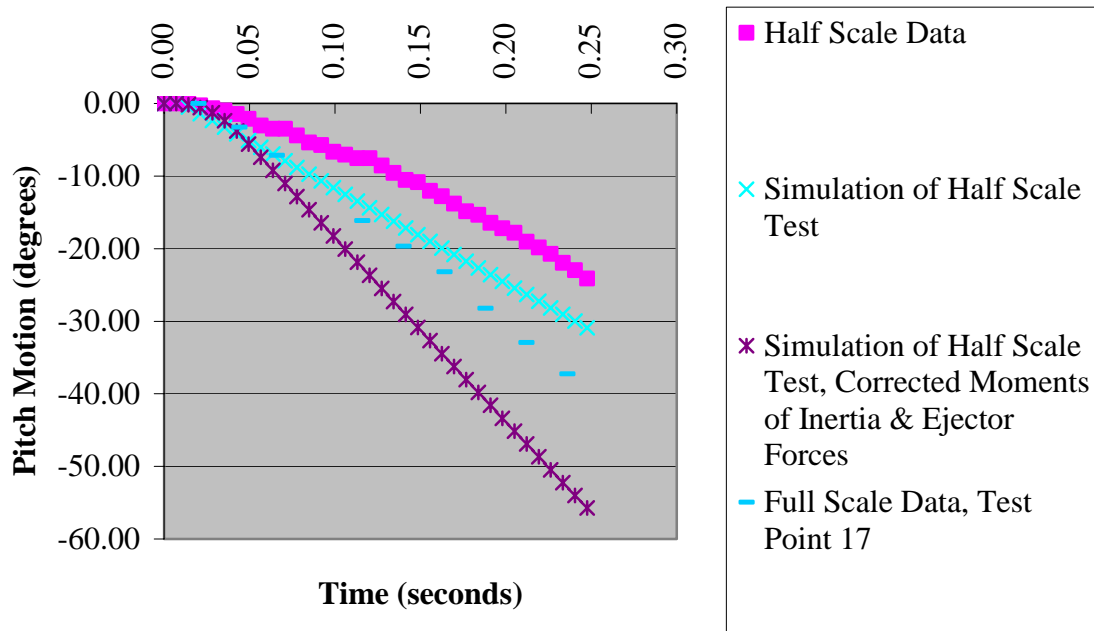


Figure H-1. Effect of Mass Moment of Inertia Plus Ejector Forces on Pitch Motion, 70 Knots Full-Scale Conditions

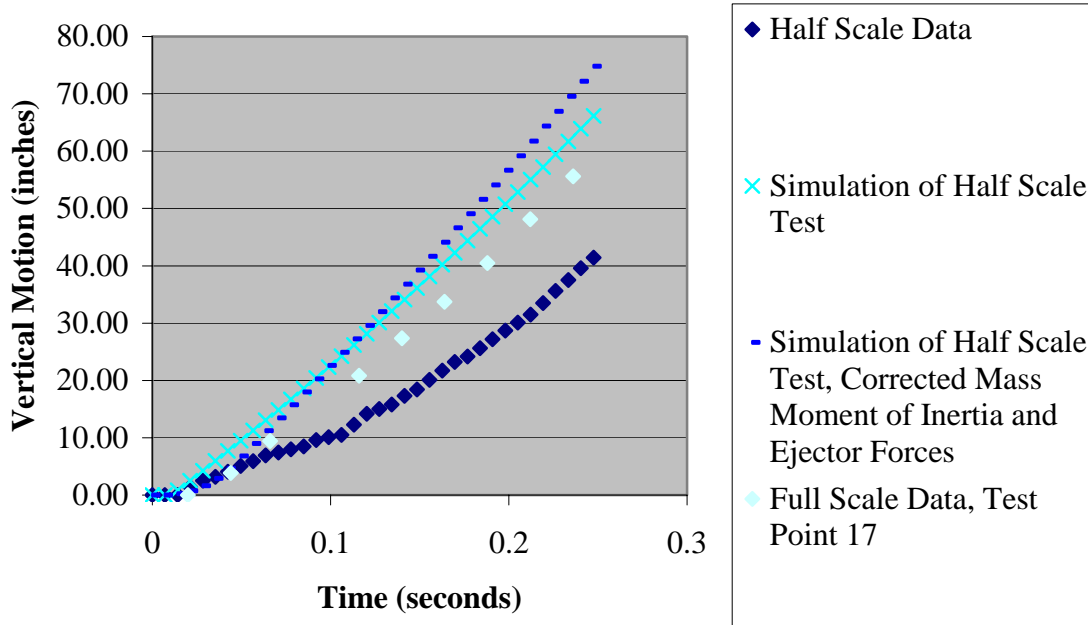


Figure H-2. Effect of Mass Moment of Inertia Plus Ejector Forces on Vertical Motion, 70 Knots Full-Scale Conditions

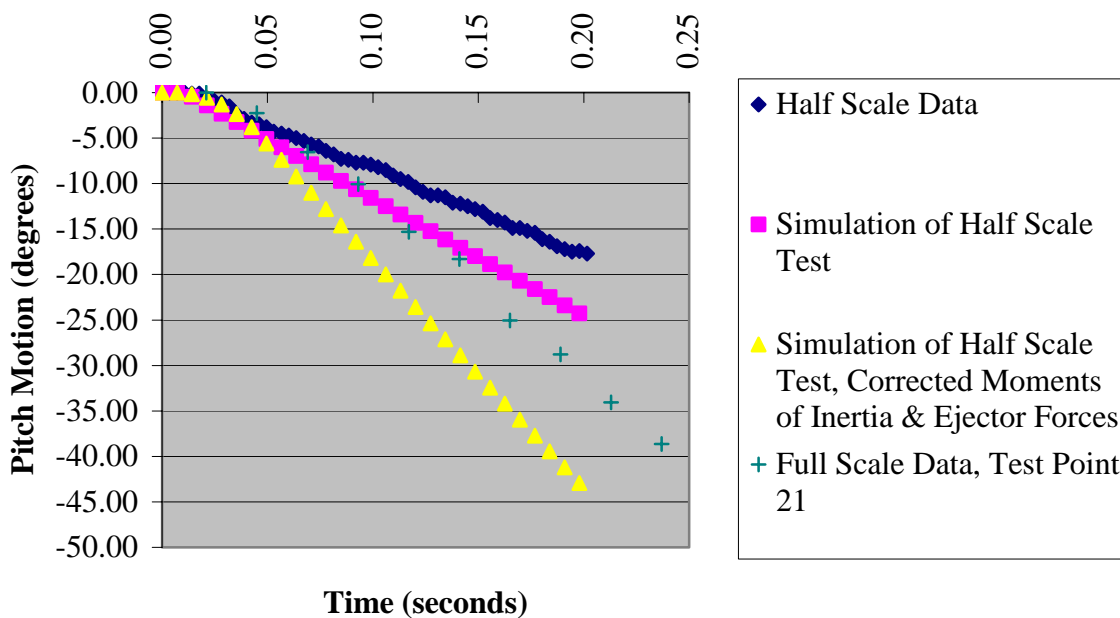


Figure H-3. Effect of Mass Moment of Inertia Plus Ejector Forces on Pitch Motion, 100 Knots Full-Scale Conditions

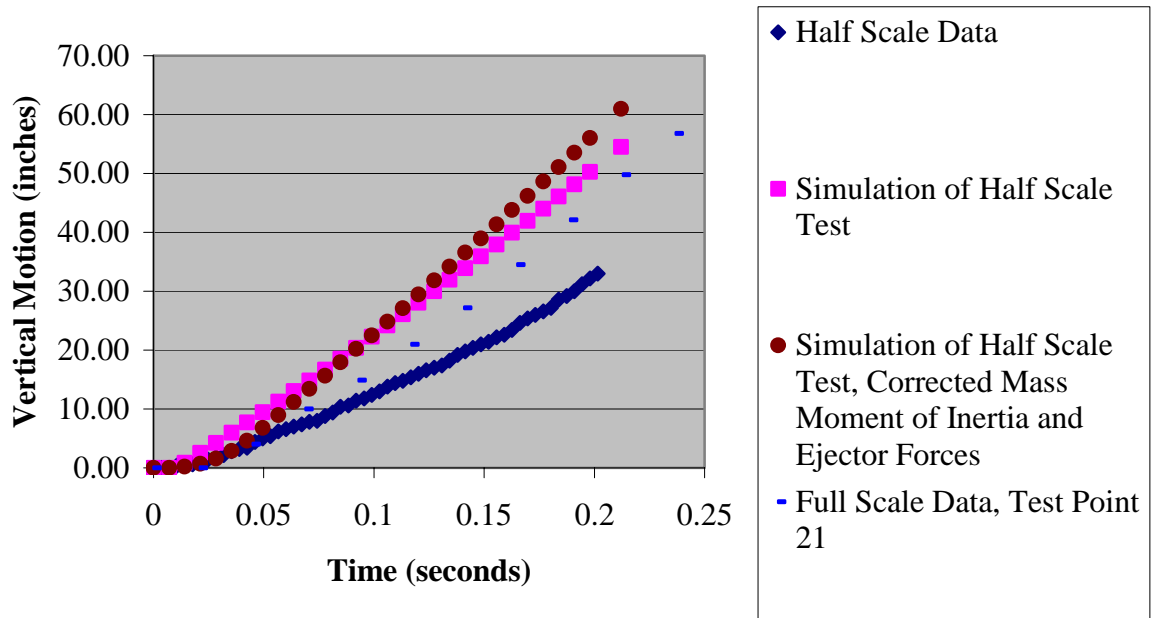


Figure H-4. Effect of Mass Moment of Inertia Plus Ejector Forces on Vertical Motion, 100 Knots Full-Scale Conditions

APPENDIX I
EFFECT OF CORRECT MASS MOMENT OF INERTIA AND EJECTOR
FORCES ON HALF SCALE TEST DATA

APPENDIX I
EFFECT OF CORRECT MASS MOMENT OF INERTIA AND EJECTOR
FORCES ON HALF SCALE TEST DATA

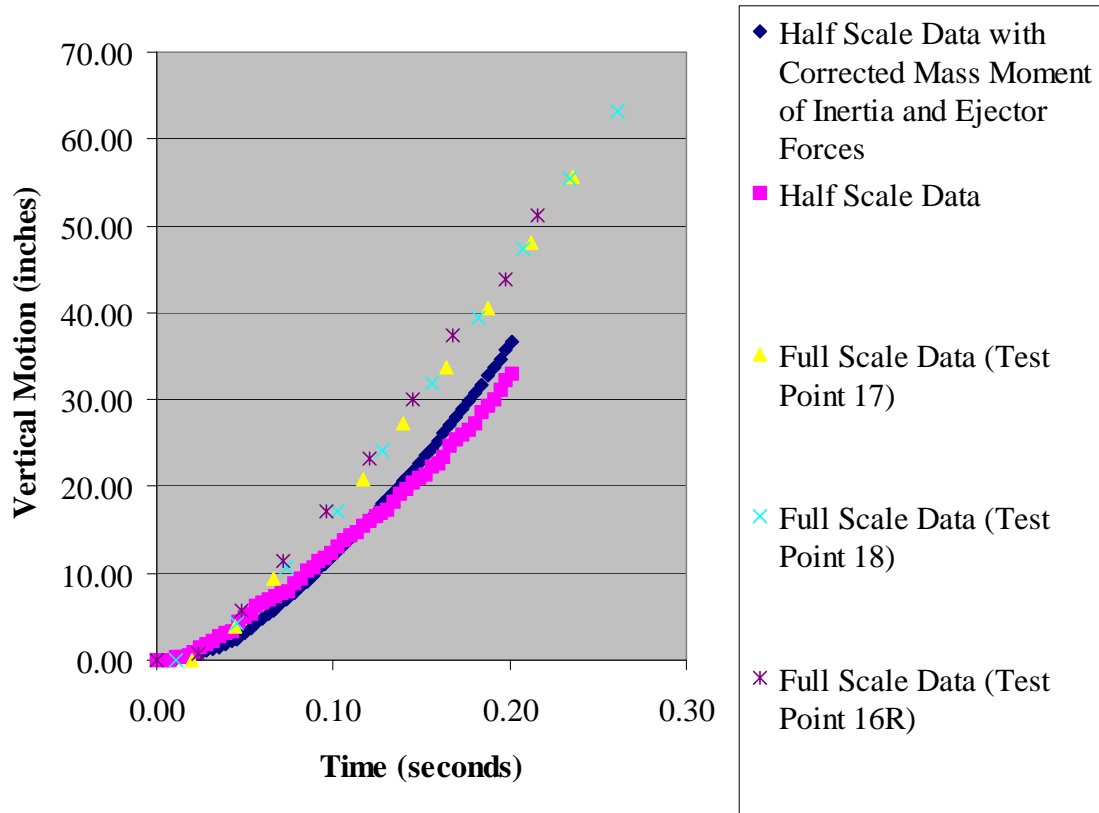


Figure I-1 Effect of Correct Mass Moment of Inertia Plus Ejector Forces on Half-Scale Vertical Motion, 70 Knots Full-Scale Conditions

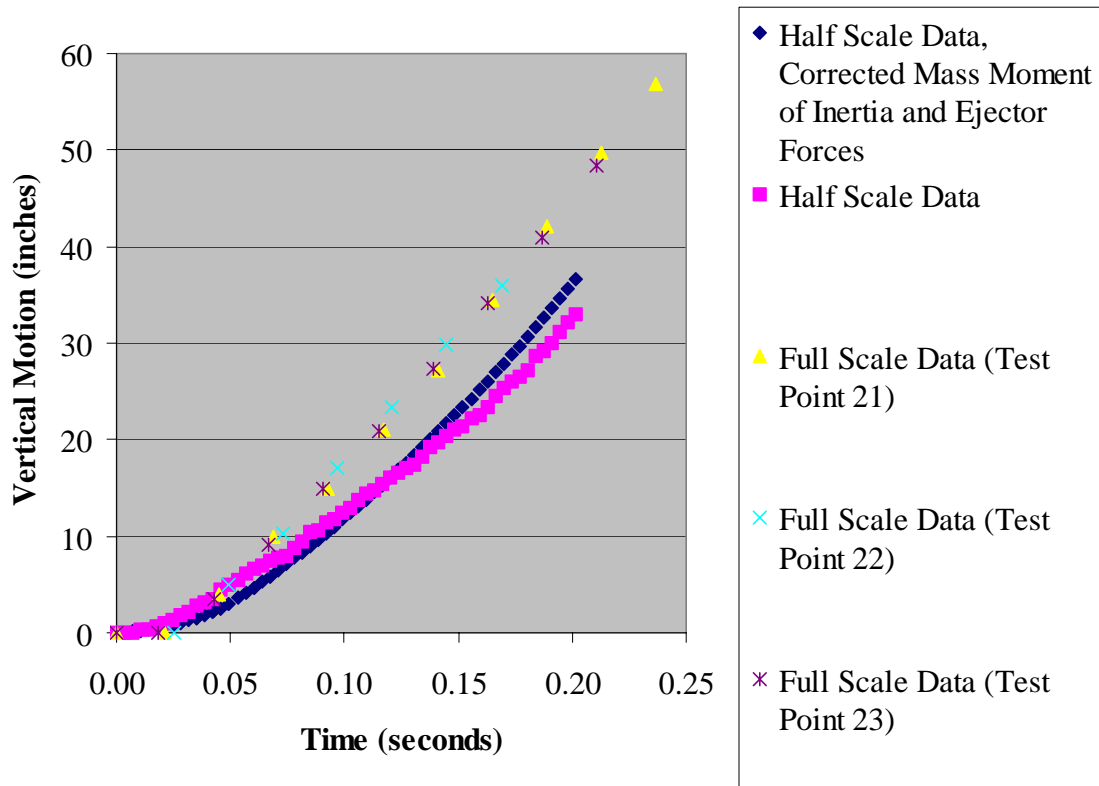


Figure I-2 Effect of Correct Mass Moment of Inertia Plus Ejector Forces on Half-Scale Vertical Motion, 100 Knots Full-Scale Conditions

INITIAL DISTRIBUTION LIST

	<u>Copies</u>
Weapon Systems Technology Information Analysis Center (WSTIAC) ATTN: Ms. Vakare Valaitis 1901 N. Beauregard Street, Suite 400 Alexandria, VA 22311-1720	1
Defense Technical Information Center 8725 John J. Kingman Rd., Suite 0944 Ft. Belvoir, VA 22060-6218	1
AMSRD-AMR	(Electronically)
AMSRD-AMR-AE-I-P-R, Dave Stephan	2
AMSRD-AMR-AE-SW, Jeff Obermark	1
AMSRD-AMR-AS-I-RSIC	2
AMSRD-AMR-PS-PI, Thomas W. Dobson, Jr.	3
AMSRD-L-G-I, Dayn Beam	1
SFAE-AV-RAH-TM, Tom Weigartz	1